**The Report Committee for Vinod Kumar Varala**

**Certifies that this is the approved version of the following report**


**Modeling of Horizontal Drilling**


**APPROVED BY**

**SUPERVISING COMMITTEE:**


**Supervisor:**

Dongmei (Maggie) Chen

Raul G. Longoria

# Modeling of Horizontal Drilling


by


**Vinod Kumar Varala, B.Tech**


# Report

Presented to the Faculty of the Graduate School of

The University of Texas at Austin

in Partial Fulfillment

of the Requirements

for the Degree of


**Master of Science in Engineering**


**The University of Texas at Austin**

**May 2016**

# Acknowledgements

# Abstract

## Modeling of Horizontal Drilling

Vinod Kumar Varala, M.S.E

The University of Texas at Austin, 2016


Supervisor:  Dongmei (Maggie) Chen

While majority of today's oil wells employ directional drilling technology (deviated, extended reach and horizontal wells), a thorough understanding of the drill string dynamics is necessary to increase the drilling efficiency. Wellbore in such wells spans long horizontal distances through the shale to extract oil and natural gas effectively. Very long slender drill pipes transmit the required torque and cutting force through miles of distance from the earth's surface to the drill bit. Drill string is subjected to different loads and torques which can cause coupled random excitations and failure of its components (drill pipes, bit, sensor tools and wellbore) eventually. If left unnoticed, these vibrations can cause stuck pipe and reduced rate of penetration, both of which are heavily cost dependent. Identifying the conditions causing harmful vibrations hence would significantly reduce cost and time.

Controlling the drill string and bottom hole assembly is one way of mitigating the dynamic instability, which is currently done by means of controlling the rotational speed, torque applied and axial force applied to the drill string. This article presents modeling of horizontal drilling and the comparison of horizontal and vertical drill string dynamics. Drill string components are discretized into lumped elements based on their curvature. A vertical wellbore structure with same drill string components is considered for comparison. The computations are performed in MATLAB. Results and discussions are presented in the later part of the report.

# Table of Contents

# LIST OF FIGURES

# LIST OF SYMBOLS

The following is the list of symbols used in the formulation of the current models.

$m$      effective mass of collars

$m_f$      added fluid mass

$\phi$      drill collar angular displacement

$k$      bending stiffness of collars

$c_h$      hydrodynamic damping coefficient

$v$      velocity of collar geometric center

$e_0$      eccentricity of the collars

$F_r$      radial contact force

$F_\theta$      frictional contact force

$J$      drill string mass moment of inertia

$k_T$      torsional stiffness

$\phi_{rt}$      rotary table angular displacement

$c_v$      viscous damping coefficient

$T$      torque-on-bit (TOB)

$R_c$      collar radius

$J_{rt}$      inertia of the rotary table

$n$      gear ratio

$J_m$      inertia of drive motor

$c_{rt}$      equivalent viscous damping coefficient

$K_m$      motor constant

$I$      current

$L$      motor inductance

$R_m$      armature resistance

$V_c$      control voltage

$m_a$      effective drill string mass

$\lambda$    wearflat length

$\kappa$    rate of change of contact/wear flat length with depth of cut

$a$    radius of the cylindrical bit

$2b$    height of the cylindrical bit

# 1.  INTRODUCTION

## 1.1 Oil and Gas

Oil and gas industry has a major role in providing the energy demands of the society. Figure 1 shows the contributions of energy sources to the world's total energy demand in 2013. Although there is a lot of emphasis on renewable energy sources, oil still contributes to close to 40% of total energy demand. This proves the significance of oil and gas in feeding the world's energy demand in current years. The United States, Saudi Arabia and Russia accounted for nearly 35% of total oil production in 2014 [1]. It is hence viable to invest large capitals in oil and gas research to produce more and more oil for reduced prices with the use of advanced technology and sophisticated equipment.
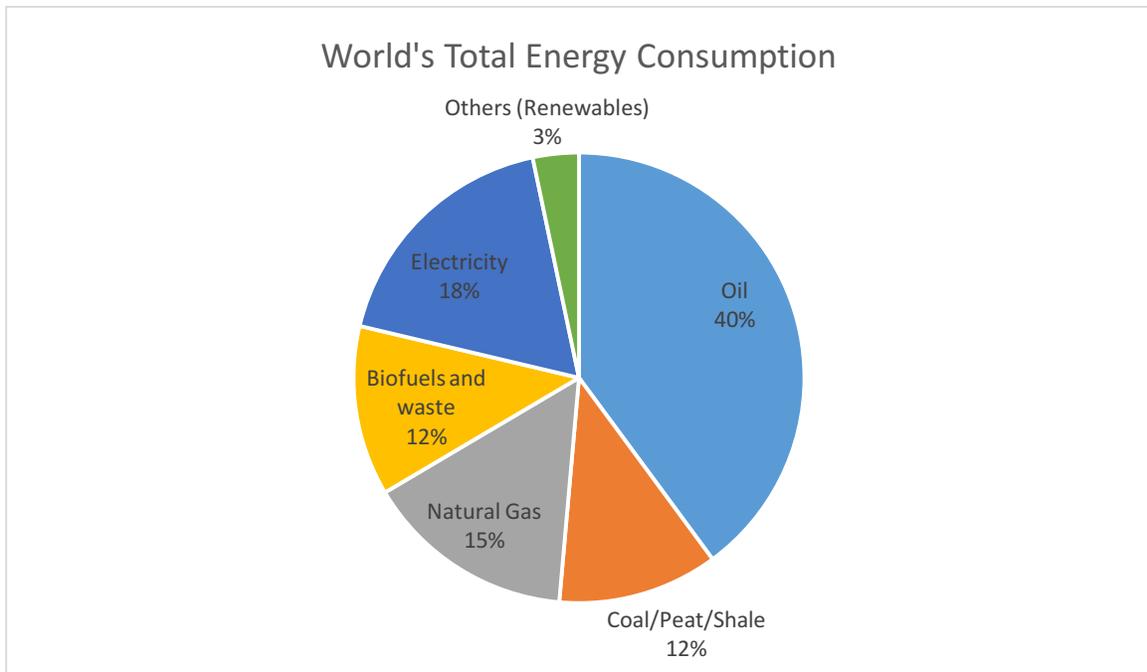


**Figure 1: World's total final energy consumption in 2013 [1]**

## 1.2 Shale gas production

Oil production in the US has ramped up since 2011 due to the advances in the fracking (hydro fracture) technology which helped in efficient hard shale gas recovery which was not possible until

then. Figure 2 shows the prediction of massive growth in the shale gas production from 2013. This shale gas deposit recovery technique also helped increase the oil production across the world to supply oil and its derived commodities for affordable prices. Figure 3 shows shale oil and shale gas reserves around the world. It can be seen that shale deposits are spread all across the world.

U.S. dry natural gas production
trillion cubic feet

billion cubic feet per day

History    2013    Projections

Shale gas and tight oil plays

Other lower 48 onshore

Tight gas

Coalbed methane

Lower 48 offshore

Alaska
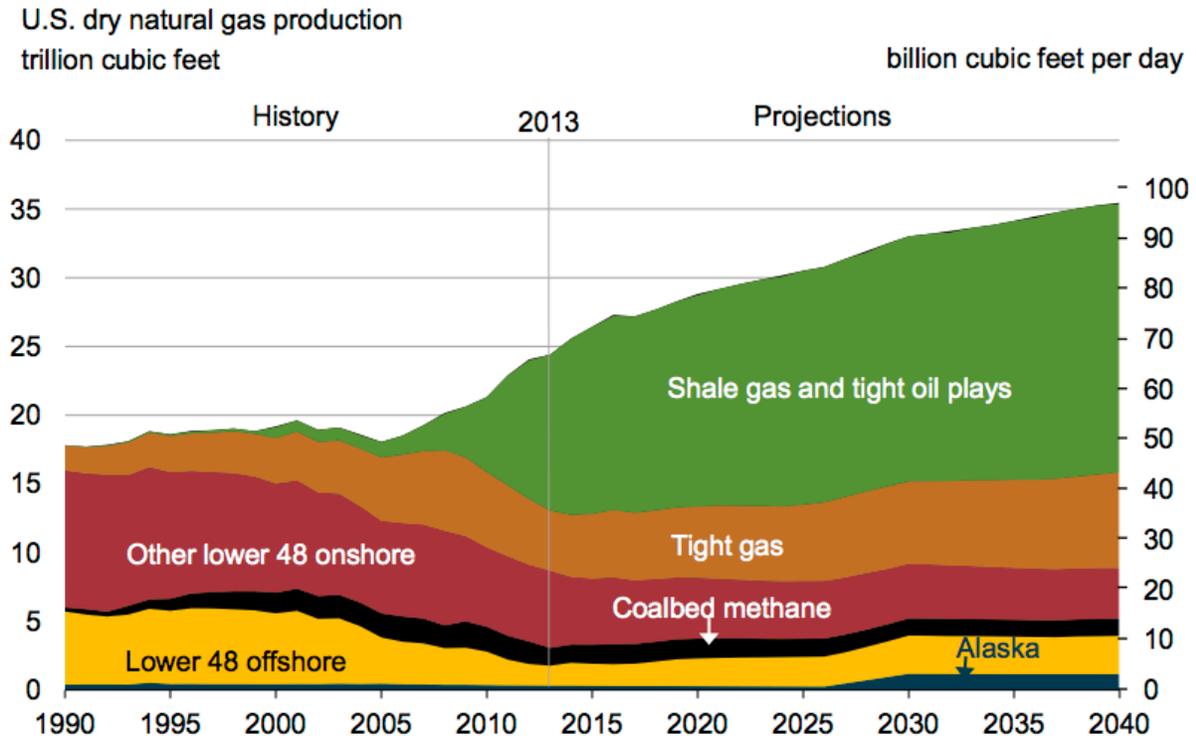
Figure 2: US dry natural gas production [2]
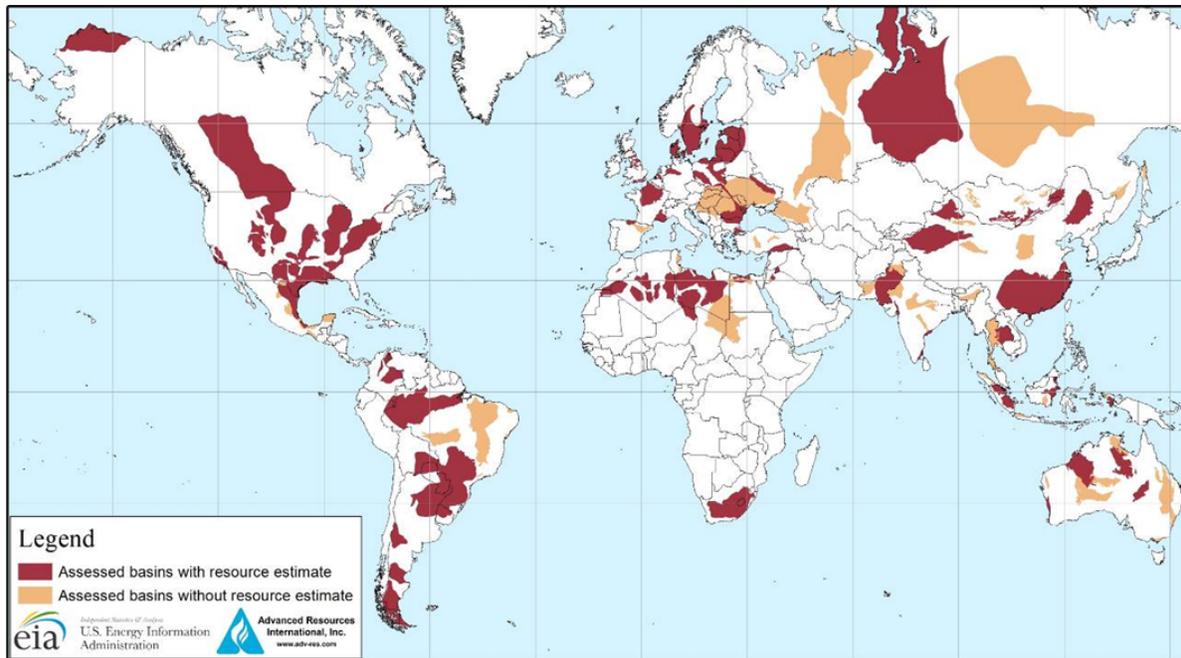
**Figure 3: Basins with assessed shale oil and shale gas formations [3]**

## 1.3 Oil Wells

Not a long ago, oil and gas was extracted extensively using typical vertical drilling wells which extended up to a few thousands of feet beneath the surface. A typical drilling system consists of top drive at the top, long connections of several drill pipes, BHA- bottom hole assembly and drill bit at the bottom as shown in Figure 4.  In recent times, because of the flexibility of the drill pipes and use of steerable systems, it is possible to steer wells in lateral directions. Hence, this makes the drill bit to move ahead in 3D space (with restrictions owing to how far the pipes can deflect laterally) and connect specific points to maximize the production volume keeping low foot print on the surface, at the same time, by not drilling too many parallel vertical wells to cover the horizontal shale reserve. This way of steering ensures intersecting multiple targets, avoiding subsurface hazards (e.g. salt, faults) and collision with other wells. Shale gas is produced primarily using directional/horizontal drilling as shown in Figure 4.

3
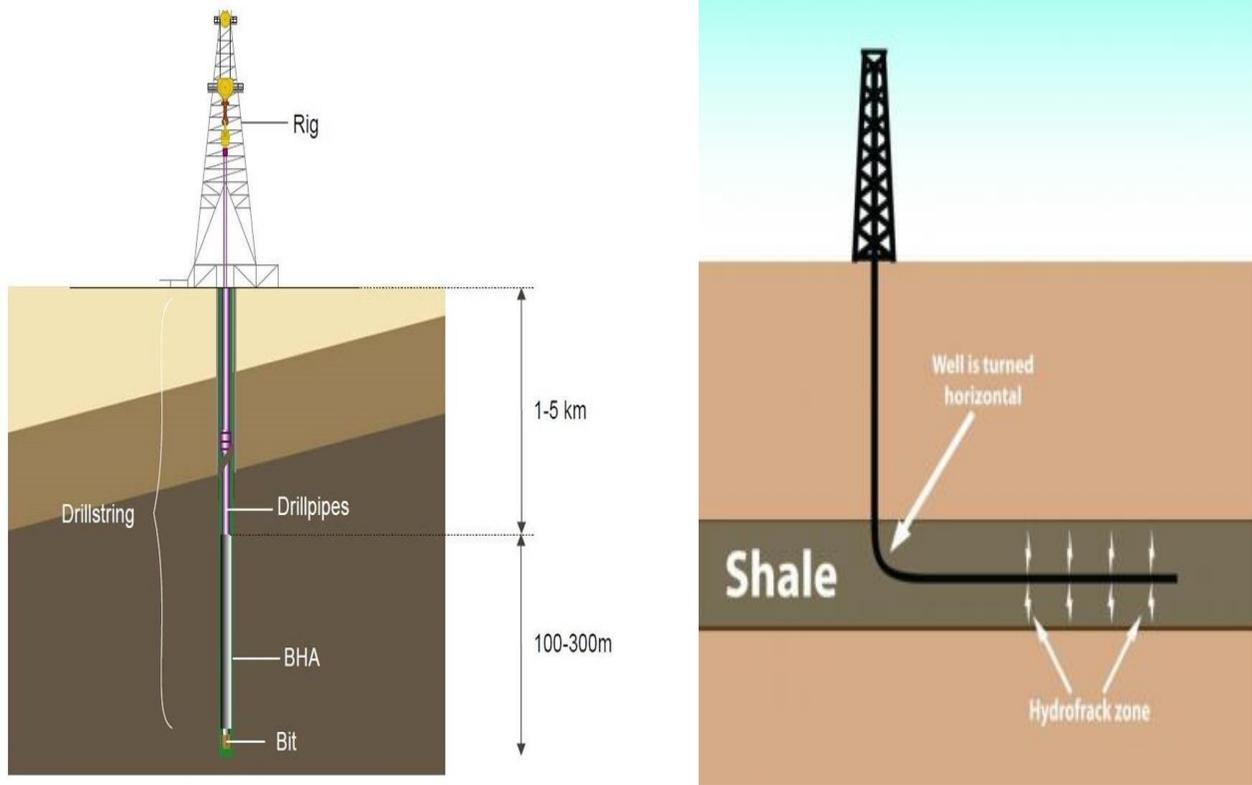
Figure 4: Traditional Vertical [4] and Horizontal drilling rigs [5]

The cost of production has been decreasing with the use of new technologies like horizontal/directional drilling, advanced downhole sensors and steerable systems. Few wells are required per square mile with directional drilling (with vertical and horizontal wellbore sections) technique, thus significantly reducing operational costs. As present production wells are being used up, exploration wells are drilled at depths as deep as 30,000 feet [6] or require drill string extended over 35,000 feet [7] in horizontal drilling. Horizontal drilling has more hydraulic fracturing impact on the horizontal shale layer and therefore more accessibility to trapped oil and natural gas, when compared to vertical drilling. It provides higher productivity and lower overall cost of production over vertical drilling. Although horizontal drilling has many advantages, it is more expensive and technically difficult to drill than vertical drilling [8].

## 1.4 Drilling System

Drilling system is a long connections of flexible drill pipes, drill subs, heavy weight drill pipes (HWDP), stabilizers, drilling motor, intrusion detection system (IDS), rotary steerable system

(RSS) and drill collars as shown in Figure 5. Drilling assembly is hoisted on a top drive which provides rotary speed, torque and hook load. These inputs at the top drive provide energy in to the system to support the weight of the drilling system and act against the friction involved in cutting. Top torque and hook load get transmitted through the long drill pipes to the bit as necessary torque on bit (TOB) and weight on bit (WOB) respectively to carry out cutting at the bit/rock interface. Effective TOB and WOB transmission determines the drilling efficiency but drill string dynamics greatly hamper the procedure.
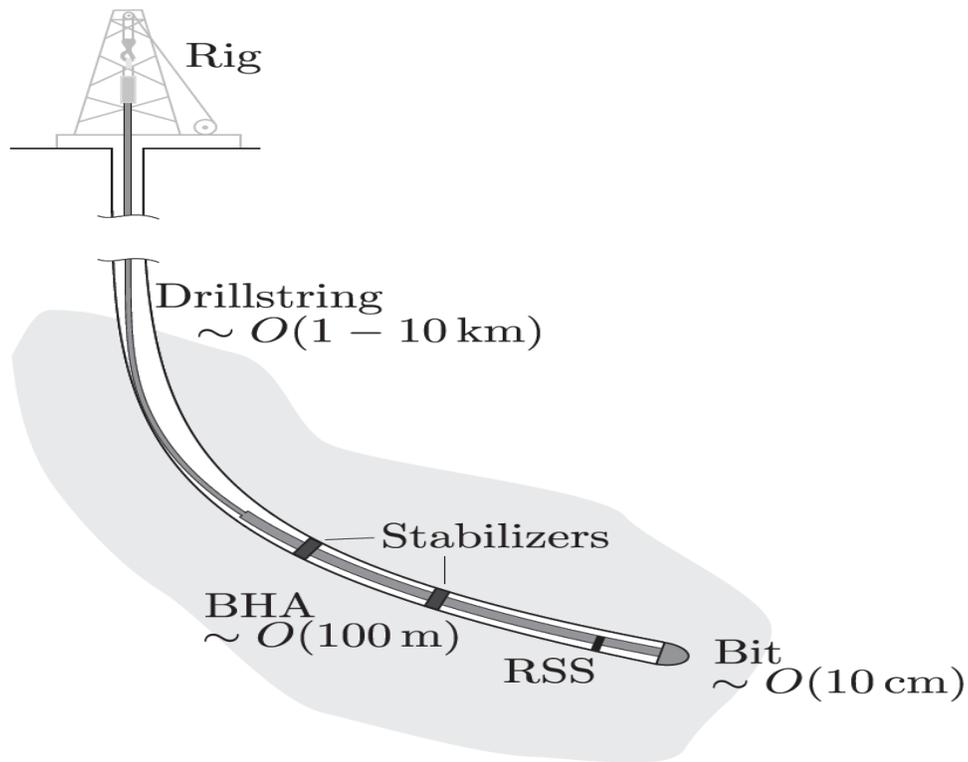
Drill string: Drill string is made up of mostly drill pipe and contains the BHA at its bottom to conduct the boring process and extract the reserves using the drill pipe. The bottom hole assembly (BHA) is the main subject for experiments. The BHA makes up the bottom region of the drill string (~ 5 % of the total length) and contains the drill bit, drilling stabilizers and drill collars. Boring operations are helped by the heavy drilling collars exerting great forces.

Bit/rock interaction: Friction on the drill bit is always a big concern, as it can decrease the life of the drill bits as well as the performance. There are various geometrical models for the drill bit cutting surfaces that help minimize the friction present while distributing the rock interaction load effectively. There are many friction models including coulomb, viscous and complex non linear (as shown in Figure 6) behaviors, to be applied to the drill string models for vibration analysis.
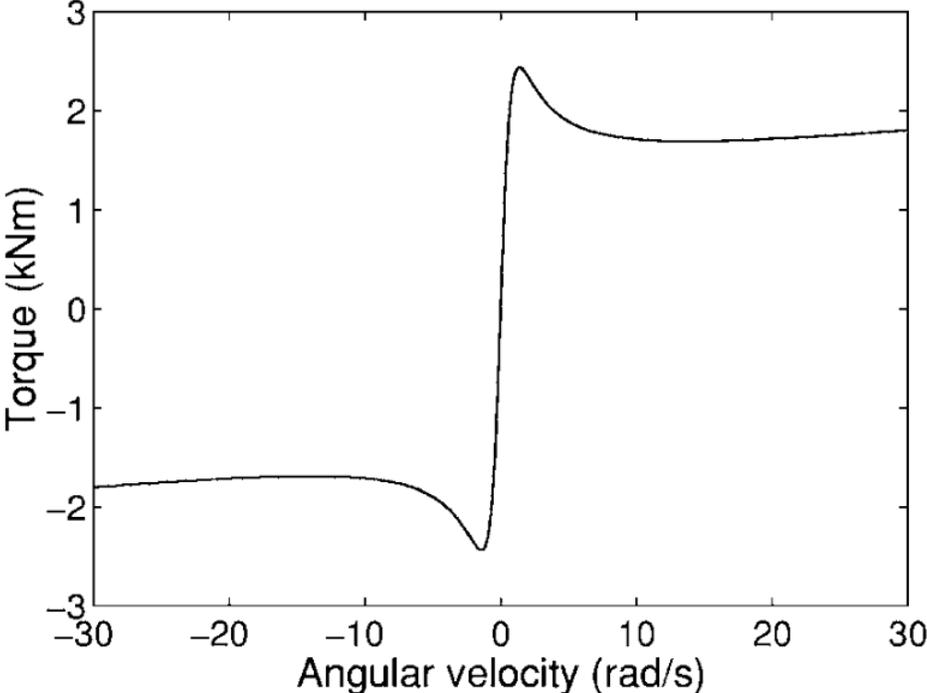


**Figure 6: Non linear frictional behavior between the bit and the formation [10]**
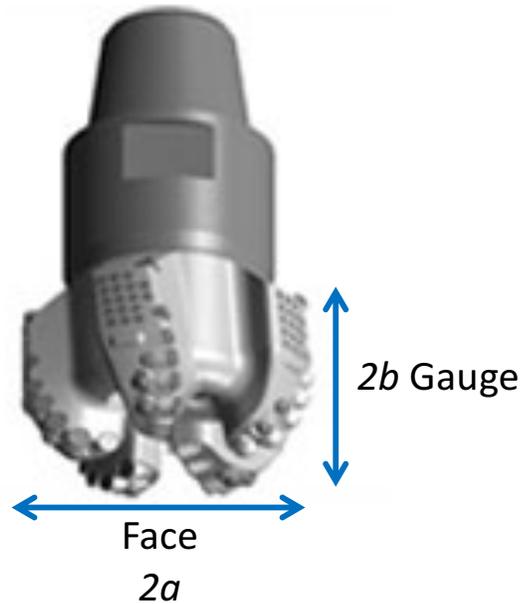
PDC with multiple blades: There are two types of polycrystalline diamond compact (PDC) cutters (1) single (which is more efficient than track cutter, however it is less stable) and (2) multiple blades (stable). In multiple blade cutter (as shown in Figure 7), blades are positioned in such a way that there are different sets of blades that cut through rock (some blades cut inner circles, other blades cut outer circles simultaneously). By using this arrangement, the force balance on the drill bit is much more stable, leading to higher efficiencies. For the model to be used in this study, a PDC with multiple blades bit will be implemented for the cutter.

Vertical Drilling System:

Although, top drive is used currently to provide inputs to the drill string, it is safe to assume that the input power is provided by DC motor with gearbox and rotary table coupling as shown in Figure 8. The gear box helps achieve different angular speeds.

As discussed above, BHA forms the bottom part of drill string and is subjected to vibrations due to the non-linear friction caused by the interaction of BHA components with the borehole wall and rock. As can be seen in the Figure 8, BHA consists of thick drill collars (for more contact area with the borehole wall in order to avoid stuck pipe situation) and stabilizers (coarsely grooved cylindrical elements of a larger diameter to avoid sticking). The lower portion of the drill collars

is generally under compression due to the heavy weight of the upper portion of the drill collars. This compressive force is referred to as weight-on-bit (WOB) in the industry.
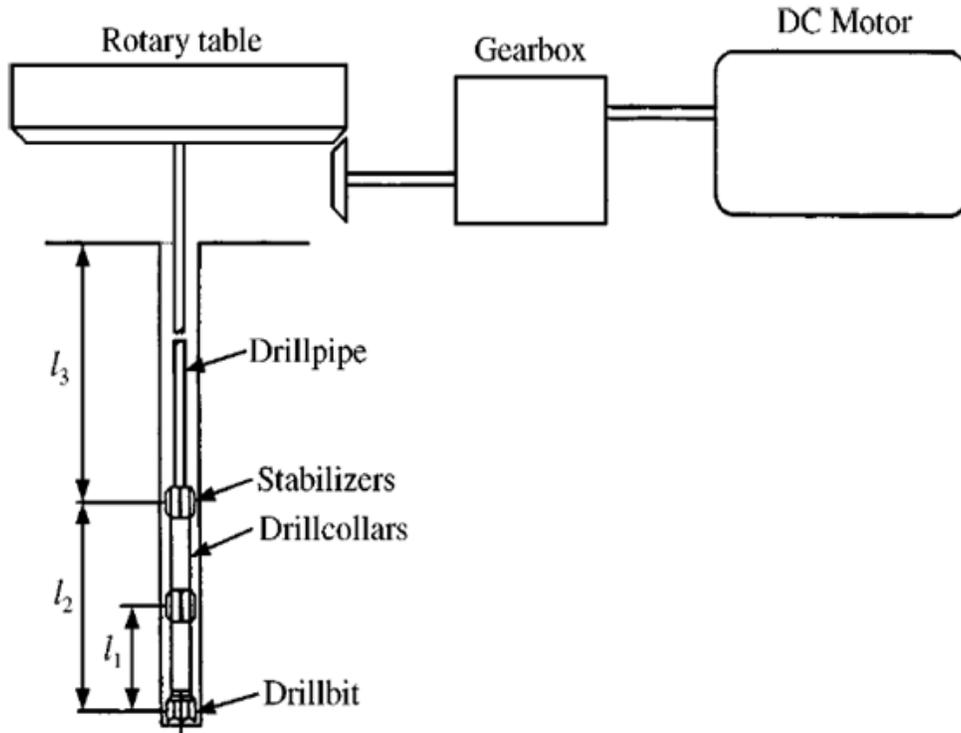


Figure 8: Vertical drilling set up [11]

Horizontal Drilling System:

Horizontal drilling with zero azimuth (2D plane) is considered in the current study. Horizontal drilling extends laterally unlike vertical drilling. Directional drilling (as shown in Figure 5) has many applications including reaching under a river, city or salt dome, intercepting (relief wells) another well at some distance away, to stop out-flow of gas at a certain depth and prevent blow outs and drilling offshore and onshore to reach out to subsea reservoirs. It starts off as a vertical well and drifts from kick off point as shown in Figure 9. The transition from vertical to horizontal drilling is gradual and has build-up, hold-on and drop-off sections. Directional drilling is also used to side track from a planned well, drill re-entry and multi-lateral wells.
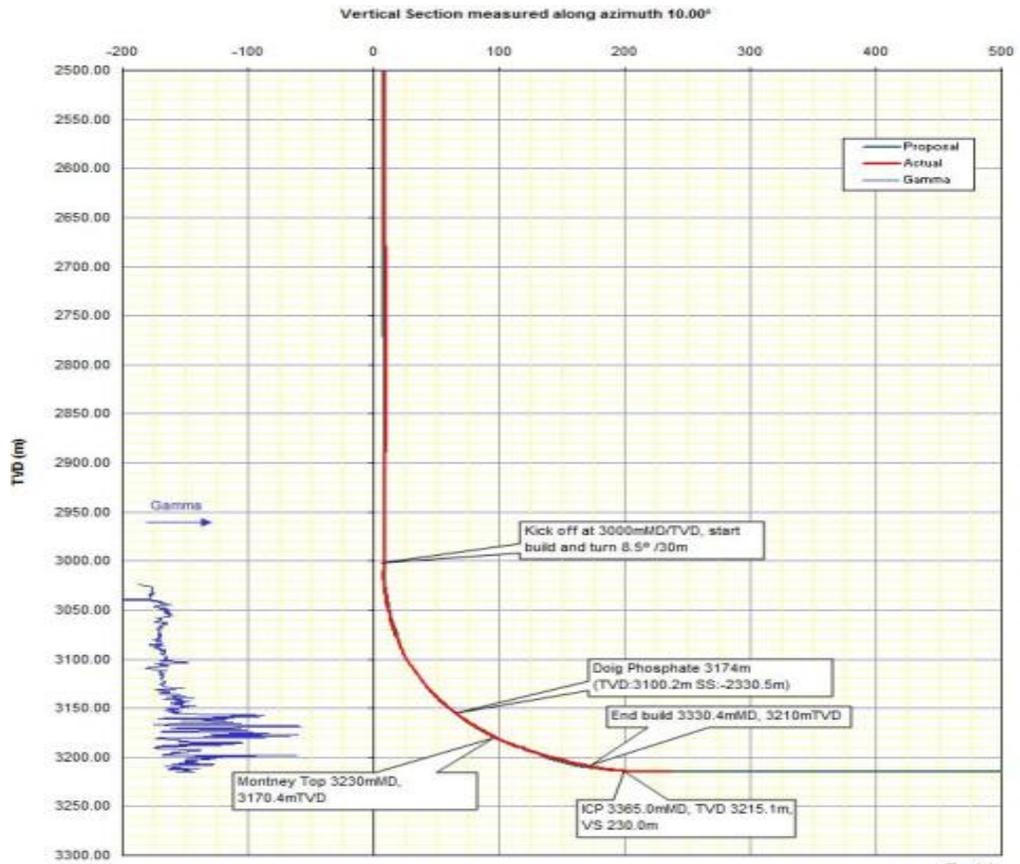
**Figure 9: Horizontal drilling set up [12]**

# 2. MOTIVATION

As already pointed out, it is very important to completely understand the drill string vibrations in order to increase the drilling efficiency by reducing harmful vibrations which cause tool and borehole damage. Vibrations are responsible for bit wear and low penetration rate. Horizontal drilling is another aspect of drilling and becoming popular in present days. The motivation for the research work comes from the following contexts.

## 2.1 Drilling Efficiency

Drilling a directional wellbore is both difficult to maneuver and control, owing to profound drill string dynamics and possibility of stuck pipe as shown in Figure 10. Stuck pipe is a situation where pipe cannot be freed from the hole without damaging the pipe. Complications related to stuck pipe cause significant cost and time. Controlling the drill string and bottom hole assembly is one way of mitigating the dynamic instability, which is currently done by means of controlling the rotational speed, torque and axial force applied at the top drive.

Drill string experiences a gradual range of tension, due to hook load at the top, in the drill pipes to compression at the bit, due to WOB as shown in Figure 11. It can be seen from Figure 11 that both vertical and horizontal drillings have a neutral point where force changes from tension to compression. Neutral point falls in the drill collar region as drill collars can take compression while drill pipes cannot handle compression due to buckling and ultimate failure. It is hence crucial to thoroughly analyze the complex drill string dynamics in mitigating severe vibrations which cause damage to drill pipes, bit, sensor tools and wellbore. As production costs go up with every extra feet of drilled pipe, stuck pipe, fish and delay, understanding the optimal rotary speeds and torques help in huge cost cuttings and increasing productivity.
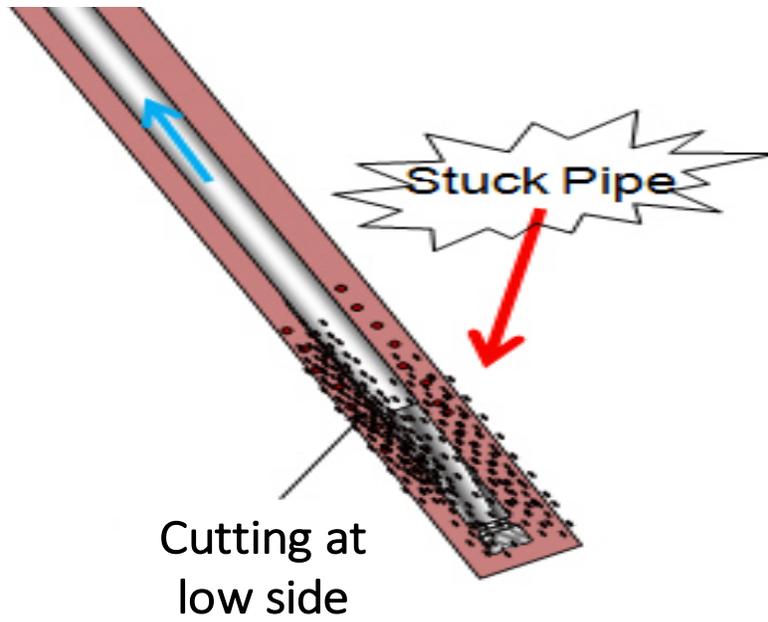
Figure 10: Stuck pipe due to irregular cutting [13]
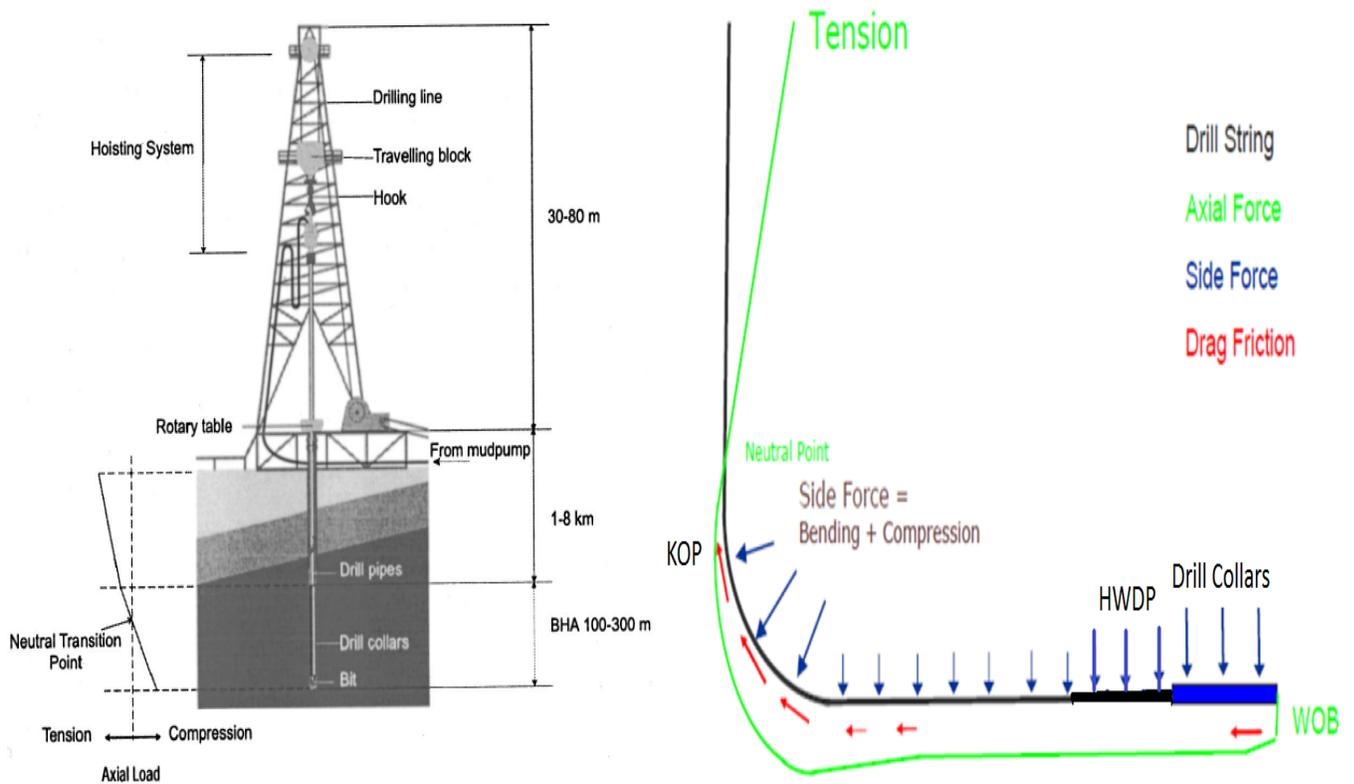


Figure 11: Tension and Compression in Vertical [14] and Horizontal [15] drilling wells

The BHA makes up the bottommost section of the drilling system (300 ft. in length). BHA is the main subject for experiments and analyses, as it is constantly under the influence of various vibrations which are broadly classified into three types- torsional, axial and lateral as shown in Figure 12. They are commonly referred to as stick-slip, bit-bounce and whirl respectively in the industry.
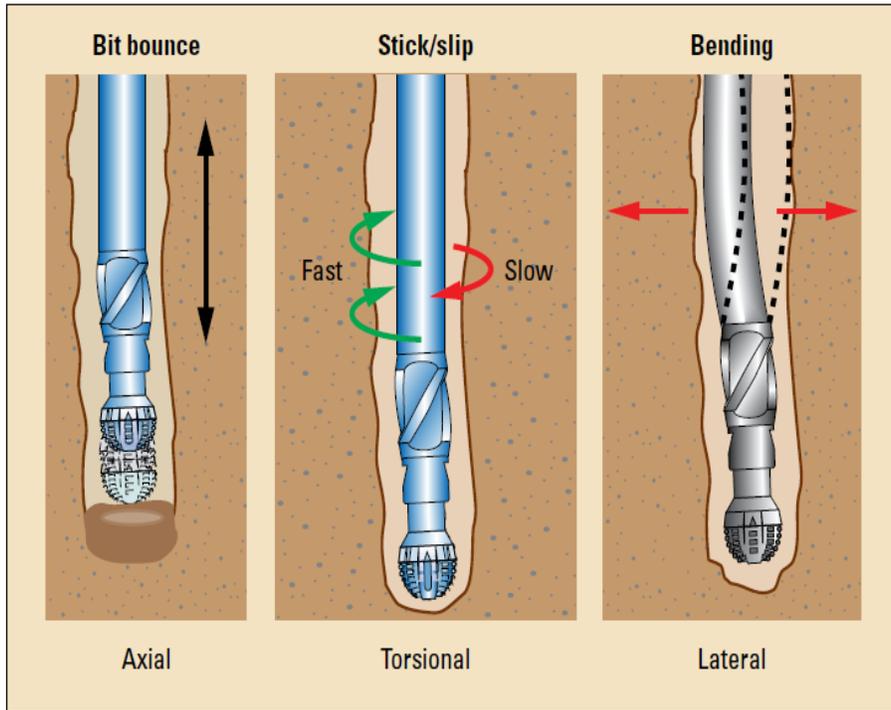


Figure 12: Different types of BHA vibrations [16]

Stick-slip: Stick-slip phases are caused by frictional forces at the bit due to insufficient cutting force. The bit stops rotating until the torque applied on the bit is high enough to overcome the rock-bit interaction forces. As the top drive continues to rotate the drill string while the bit being stuck, the entire drilling system twists and store energy. Once sufficient torque is available to overcome the rock-bit interaction forces, the bit releases and rotates faster than top drive speed until the twists in the drilling system is removed causing the applied torque on the bit to fall below the cutting limit and stopping the bit once more. This cycle repeats, typically at a frequency of about 0.5 to 2 Hz as shown in Figure 13. This violent rotation releases a lot of energy which causes axial and lateral vibrations. Field data suggests that these torsional vibrations can go as high as 250 Hz.
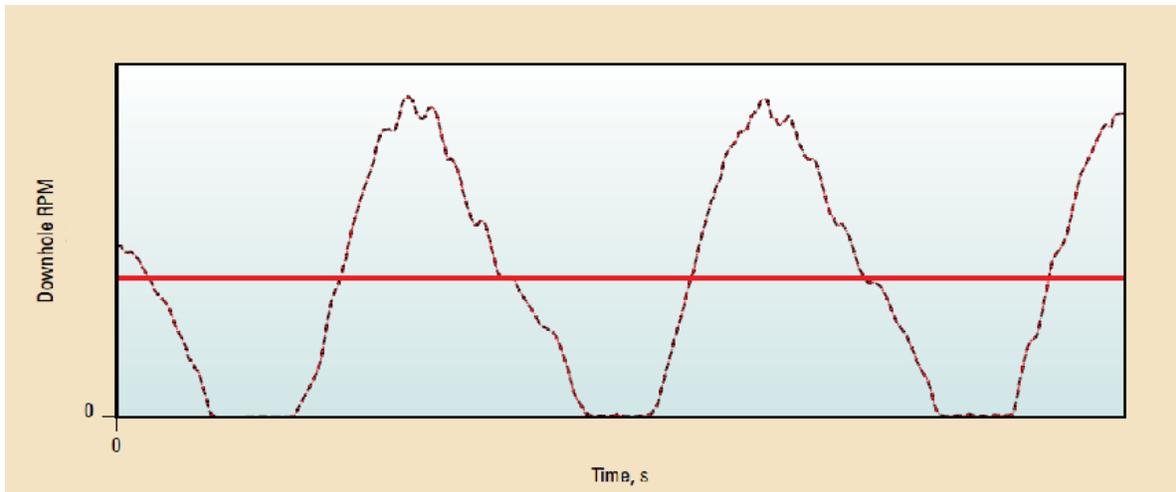
**Figure 13: Fully developed Stick-slip [16]**

Whirl: Lateral vibrations are manifested as whirl. Whirling of the drilling system occurs when the axis of rotation of the drilling system moves within the borehole. Whirling within the drilling system is acceptable but in most cases the whirling of the drilling system begins to impact the borehole wall, causing damage to the drilling system structure.

Forward whirl occurs when the whirl is in the direction of the drill string. In regular forward whirl, drill string comes in contact with the borehole wall at same spots leading to excessive wear. Backward whirl occurs when the two rotations are opposite to each. Generally, backward whirl causes severe wear than forward whirl. Both forward and backward whirls are shown in Figure 14. Chaotic whirl is characterized by both forward and backward whirls involving erratic lateral movement with high shock loads. Whirl is difficult to detect at the top as the magnitude of vibrations are damped by the viscous mud up the drill string.

13
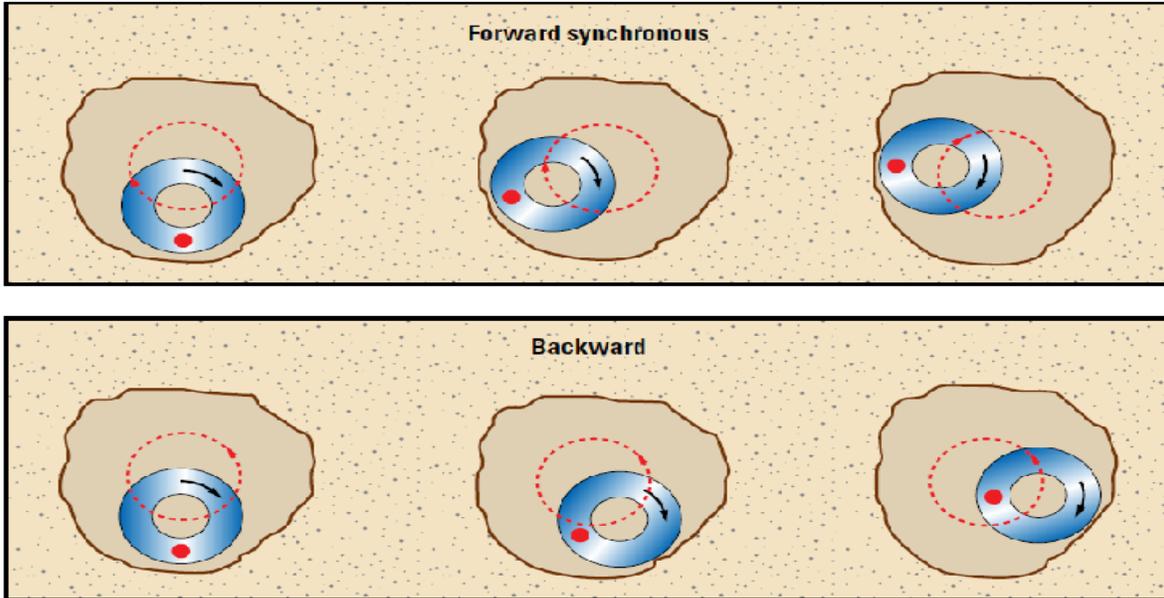
**Figure 14: Types of whirl [16]**

Bit-bounce: Axial vibrations cause bit-bounce. Some of released energy from the torsional vibrations manifest into axial vibrations. They are also sometimes caused by the agitator tools which are employed to increase rate of penetration (ROP) by applying a small impulse whenever required. During these vibrations, bit looses contact with the rock surface at bottom of bit.

All these vibrations are generally coupled together among each other and often tend to be chaotic. They are detrimental to the drilling system and cause severe damage to the sensor tools and sometimes may cause unscrewing of the drill pipe connections. Drilling elements may ultimately fail due to the fatigue caused by these vibrations. It is hence important to model the BHA and analyze the vibrations arising out of the bit/rock interactions.

## 2.2 Directionality

Horizontal wells are becoming more and more popular these days. More than 60% of the on-shore wells in the United States as shown in Figure 15 and more than 80% of the wells in Oman, Qatar and Abu Dhabi are horizontal [8]. For a successful horizontal well, it is necessary to understand drill string dynamics in order to predict the directional response of the BHA. This study also helps in understanding the shape of the borehole and hence in the directional control.

14

**Well Type - Rotary Rig Count**
**United States**

January 1997 - August 7, 2015
Source: Baker Hughes, WTRG Economics

WTRG Economics © 2015
www.wtrg.com
(479) 293-4081

Horizontal    Directional    Vertical
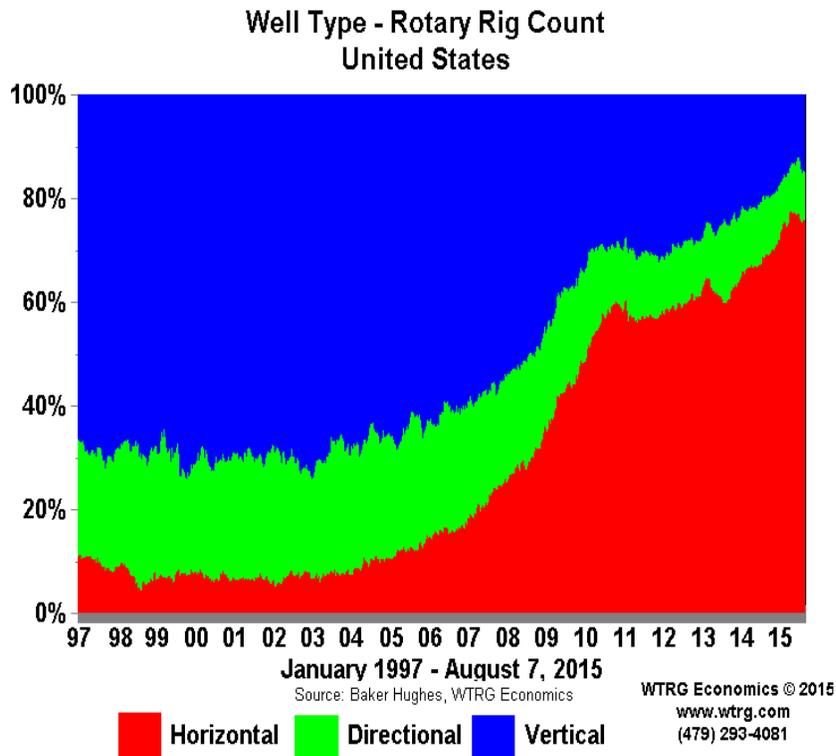
**Figure 15: Different types of wells over time [17]**

## 2.3 Control and Automation

As the industry is steering towards Automation, understanding the drilling system model is a crucial step for achieving Automation. Drill string dynamics model forms an integrated piece in understanding the response of the drilling system for given inputs at the top. Figure 16 shows how changing the input parameters (like weight on bit (WOB) and top drive RPM) lead to achieving minimal/no vibrations zone. This is the central idea of any control design- to understand undesirable regions and steer away from those regions. Figure 16 shows a basic BHA control. In industry this is achieved by rotary steerable systems (RSS) which employ point the bit and push the bit strategies to steer the well.
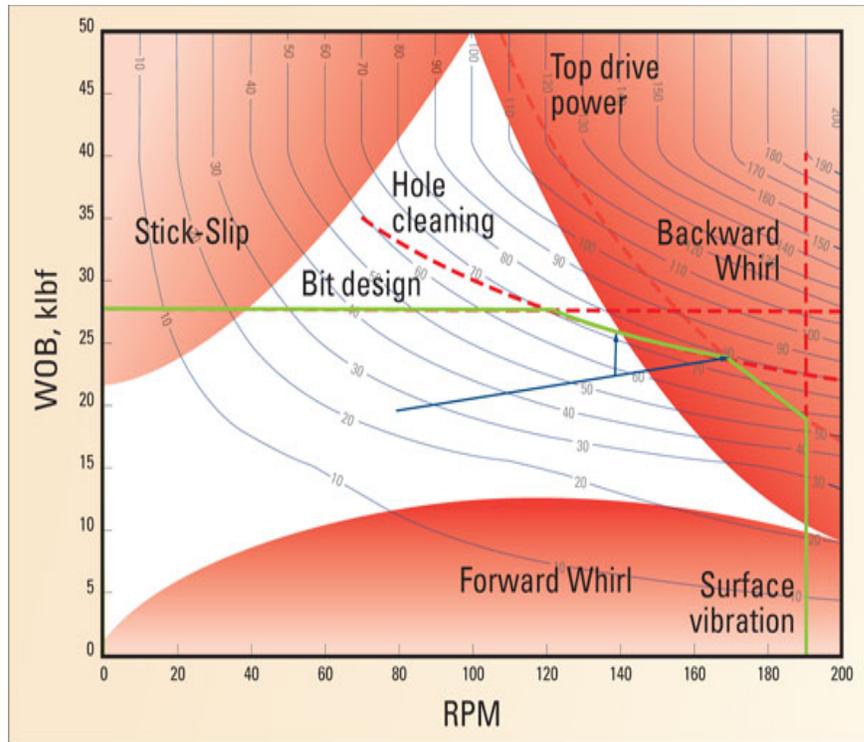
Figure 16: Regions of vibrations [18]

Although there are various models for vertical drilling in literature, comparison of vertical and horizontal drilling dynamics is not studied yet. Current study primarily focuses to address this issue.

# 3. LITERATURE REVIEW

## 3.1 Drill string formulation

Research on vertical drilling started in the early 1970s and is still in progress. Drill string can be fairly assumed to be a long flexible beam. Inputs at the top and rock cutting at the bottom form boundary conditions to the beam. This long beam can be analyzed in various ways including approximating it to a one mass, two mass and multiple mass lumped systems. Various modeling approaches are tried including theoretical, experimental, FEA, Runga-Kutta simulation and field experiments.

One of the early articles on drill string formulation is by Bailey and Finne [19]. They developed simple dynamic mathematical models of drill string to understand and mitigate vibrations as well as to verify them with experimental results but with limited insight. Halsey et al [20] modeled stick-slip phenomena and torque feedback to study and cure stick-slip oscillations. But, their one degree of freedom model could not predict occurrences of stick-slip under given sets of condition.

Apostal et al [21] developed an FEA model to study the effect of damping (presence of fluid, formation, friction, other effects) on forced frequency response models of BHA vibrations. The FEA model assumes cyclic behavior of drill string which is not a real situation downhole. Spanos et al [22] studied complex dynamics of drill string behavior using frequency response models. They were unable to reproduce the observed dynamics phenomena though their model provides qualitative analysis of BHA performance. The model also does not consider stiffness and excitation of BHA components.

Brett et al [23] assumed constant drill string friction torque and standard relationship between drill string stiffness and BHA inertia for their model which shows that the bit-rock interaction initiates the torsional vibrations. The model uses Runge-Kutta computational scheme for simulation. Dykstra et al [24] developed a model to study mass imbalance which results in the cause of lateral vibrations and compared the results with experimental studies. The model restricts to determine the deflection in drill string at different rotary speed and does not predict the dynamic behavior.

Jansen et al [25] developed 2 degrees of freedom (DOF) - torsional and axial model to mitigate torsional vibrations using active damping system for a drill string driven by electric motor as well as hydraulic motor. Menand et al [26] modeled drill pipe as a soft string and BHA as a stiff string with contacts between drill string and wellbore modeled as a nonlinear spring. This full 6 DOF model can be used in real time drilling operation as it does not use FEA. The effect of temperature is also considered.

Christoforou et al [11] studied fully coupled vibrations of actively controlled drill strings. They modeled the drill string as a single mode approximation of a continuous beam model that is allowed to rotate off-center within circular wellbore. Only 4 DOF - 3 translational and 1 rotational about the axis of drill string, are studied with other 2 DOF assumed to be insignificant. Mihajlovic et al [27] studied the interaction between torsional and lateral vibrations in flexible rotor systems with discontinuous friction. They presented additional modeling and experimental work of rotating unbalanced masses, further confirming the drill string behavior under stick-slip and whirl.

Navarro-Lopez et al [28] performed dynamical analysis to avoid harmful oscillations in a drill string. They presented a single lumped mass model to look at stick-slip and used this model to create a sliding controller to mitigate its occurrence. Navarro-Lopez [29] developed an alternative characterization of bit sticking phenomena in a multi-degree-of-freedom controlled drill string. A simple lumped mass model was used to look at stick-slip.

Rudat et al [30] performed model-based stability analysis of torsional drill string oscillations. They used single degree of freedom model to investigate stick-slip. In 2012, Liao et al [31] detailed several experiments applied directly to a BHA. Two different regimes are observed: periodic bump and stick, or continuous rolling motion. Patil et al [32] published a comparative review of modeling and controlling torsional vibrations and experimentation using laboratory setups. The focus was on torsional vibrations which manifest in to stick-slip.

Nandakumar et al [33] presented a modified 2 DOF freedom lumped mass model to look at stick-slip and bit bounce. They observed that many previous models do not allow for sufficient damping of axial and torsional vibrations within the drill string due to material properties.

Various other articles developed control-based models to employ different control techniques including simple PID [11], H-Infinity [34], [35], Non-Linear control (sliding mode [36]) and semi discretization (state delay differential equations) [37].

## 3.2 Bit/rock interaction

Modeling and analyzing drilling system vibrations require thorough understanding of bit/rock interaction. The study of bit/rock interactions requires understanding the relationship of cutting and frictional forces with cutting velocity and depth of cut. Different types of approaches were employed to formulate bit/rock interactions. They include FEA (LS- DYNA, ABAQUS- Explicit and FLAC), phenomenological, empirical and analytical approaches.

Early works on cutter/rock interaction dates back to 1950s. Fairhurst authored a series of research papers in mid 1950s. Fairhurst et al [38] along with others ([39], [40], [41]) proposed that two simultaneous mechanisms (cutting and friction) are operative in the analysis of single cutter interaction with the rock. Feenstra ([42], [43]) wrote the issues associated with the emerging PDC cutters and emphasized the importance of research on PDC bit in 1988 when the oil prices collapsed. Active research on PDC bits received attraction since then.

In 1992, Detournay et al [44] studied the interaction of PDC bit with the rock (ductile failure mechanism) by a series of experiments both on single cutter cutting and PDC bit cutting and established rate-independent interface laws. Following previous work ([38], [39], [40], [41]), Detournay phenomologically developed friction and cutting components of both torque-on-bit and weight-on-bit [38]. Detournay et al established 3 DOF [45] and 5 DOF [46] directional drilling models based on his phenomological model.

Che et al [47] developed analytical three dimensional quasi orthogonal cutting model based on Nishimatsu's [48] two dimensional orthogonal cutting theory (brittle failure mechanism) for brittle

19

rocks. Gerbaud et al [49] presented a new cutter rock interaction model which includes build-up edge of crushed materials on the cutting face, effect of chamfer angle, forces on the back of the cutter and back flow of crushed materials. All of these models (Detournay, Che and Gerbaud) have been proved experimentally for the single cutter interactions.

Different methods of establishing relationship between forces and penetrations, including Distinct Element method (DEM) by Akbari in 2011 [50], Finite Element Tool LS-DYNA by Zhou in 2013 [51] and empirical model by Glowka in 1989 [52] were studied. Analogies of bit/rock interactions with the metal cutting process were explored by Che et al [53] in 2012.

All of Detournay's models ([45], [46]) are derived using interface laws averaged over one revolution of the bit. His models are hybrid models (static and dynamic). Frictional forces are considered to be constant in his formulation. This formulation works for building steady state models but doesn't work for dynamic models where the vibrations, including torsional vibrations, may go up to few hundred Hzs in which case steady state models fail to capture the root cause of the observed high frequency content.

Though there are many vertical drill string models, only few horizontal models are available in the literature. Current study explores horizontal drilling models to study drill string dynamics. Bit/rock interaction used in this model is primarily based on phenomenological model (which is widely followed in the industry) developed by Detournay [44] in 1992.

# 4. MODELING ASSUMPTIONS

The following assumptions are made for the modeling procedure.

1. BHA is assumed to be a lumped mass with both axial and lateral vibration, whereas the rest of the drill string bottom-up is assumed to be undergoing only axial vibration. This assumption is justified since stabilizers at the top of the BHA restrict lateral movement and the lateral motion of drill pipes has insignificant effect on the BHA vibrations. Thus, BHA is assumed to be a cantilever beam (modeled as Rayleigh beam) with stabilizer as the fixed end and lumped collar mass at the free end. The lateral vibration of BHA is confined within the borehole.

2. Horizontal drilling modeling is done slightly different. Each section was assumed to be a lumped mass (with stiffness). Vertical, build-up, hold-on, second build-up, horizontal and BHA sections were assumed lumped masses individually. As with vertical section, horizontal BHA is also assumed to be a cantilever beam (modeled as Rayleigh beam) with stabilizer as the fixed end and lumped collar mass at the free end. Also, BHA is assumed to undergo both axial and lateral vibration, whereas the rest of the drill string is assumed to be undergoing only axial vibration.

3. The drill pipes are assumed to be a hollow cylinder rotating about longitudinal z-axis with a constant angular speed. As drill pipes are flexible to torsion about their axis, the torsional deflection in drill pipes is considered significant. Whereas, the torsional deformation in collars is negligible as they are stiff enough to resist torsion.

4. BHA in each case has six states – $[\theta, \phi, r, \dot{\theta}, \dot{\phi}, \dot{r}]$. $r, \theta$ correspond to polar co-ordinates in the lateral direction and $\phi$ corresponds to torsional deflection about BHA's axis as shown in Figure 18. Whereas, drill string on the other hand has only two states $[x, \dot{x}]$. $x$ and $\dot{x}$ are axial displacement and velocity respectively.

5. Polycrystalline diamond compact (PDC) bit is assumed in the analysis. Multiple blades (six blade) bit will be implemented for the cutter. Cutting takes place in ductile mode with depths of cut ranging from 0.1 to 2mm, which typically are the depths of cut encountered

in drilling applications [44]. Bit is always assumed to be tangent to the borehole path for the sake of simplicity. Rock is assumed to be isotropic.

# 5.   MODELING

## 5.1 Vertical Drilling System
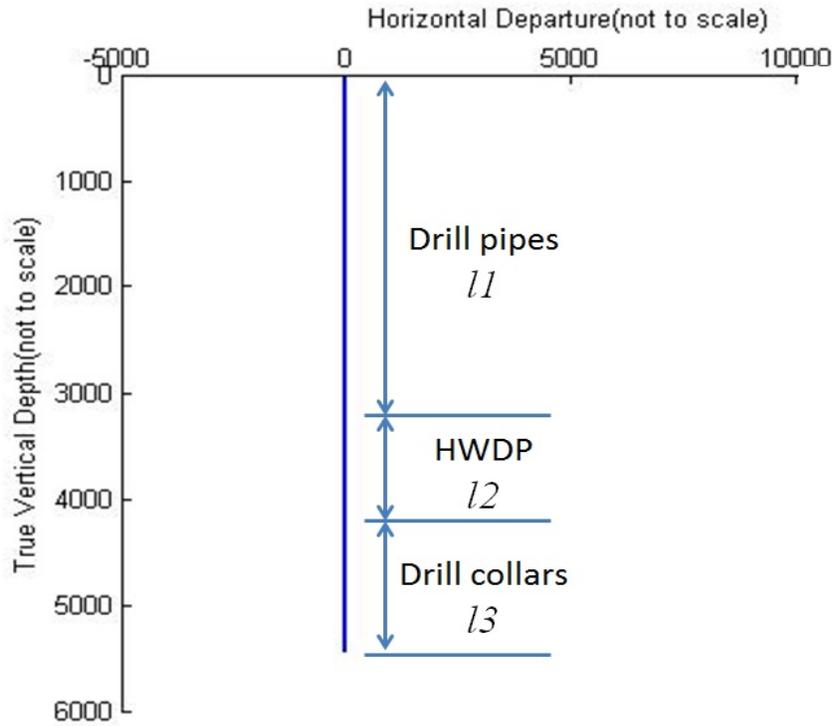


**Figure 17: Vertical Drilling System Layout**

Past experiments have explored the dynamics of the BHA making certain assumptions that either couple or decouple the dynamics of lateral, torsional, and axial vibrations. Dykstra et al [54] presents a 4 DOF model (2 lateral, 1 axial and 1 torsional) that implements shear beam theory on the BHA to develop the equations of motion. During the development of the BHA model, the following assumption was made: the deflections are small that any bending produced in one axis does not affect other axes [11]**.** Thus, they were able to decouple axial, rotational and lateral vibrations using shear beam theory. Bit/rock interactions and drill string dynamics are implemented based on a previous Christoforou's model [11].

The current work follows Christoforou's model [11] for vertical drilling modeling. In this model, a fully coupled, axial, lateral, rotational, and torsional vibration model of the entire drill string is developed using a lumped parameter approach. However, due to the stabilizers on the BHA, its lateral vibrations are decoupled from the upper drill string vibrations. For the bit/rock interactions, bit and rock formation characteristics are used to determine the WOB, which in turn is used to find the TOB. An assumption made by Christoforou [11] regarding the stabilized sections of the drill string allows the BHA to be modeled as a simply supported beam for traverse motion. As discussed, BHA has six states – $[\,\theta, \phi, r, \dot{\theta}, \dot{\phi}, \dot{r}\,]$. $r$, $\theta$ correspond to polar co-ordinates in the lateral direction and $\phi$ corresponds to torsional deflection about BHA's axis as shown in Figure 18. Whereas, drill string on the other hand has only two states $[x, \dot{x}]$. $x$ and $\dot{x}$ are axial displacement and velocity respectively. The equations of motion for the fully coupled drilling system (and BHA as shown in Figure 18) based on Christoforou [11] are shown as follows.
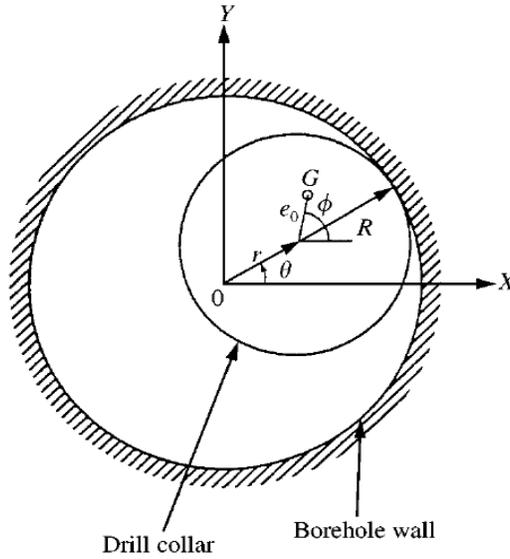


Figure 18: BHA layout within borehole wall [11]

BHA has centripetal and radial accelerations in r direction. This comes from the imbalance force due to the eccentricity, restoring force (due to lateral stiffness) and hydraulic viscous damping as given below.

$$\left(m + m_f\right)\left(\ddot{r} - r\dot{\theta}^2\right) + k\left(x, \phi, \dot{\phi}\right)r + c_h|v|\dot{r}$$
$$= \left(m + m_f\right)e_0\left[\dot{\phi}^2 \cos(\phi - \theta) + \ddot{\phi}\sin(\phi - \theta)\right] - F_r$$

where $F_r$ is the radial force coming from the wellbore when there is a contact. Similarly, tangential acceleration in $\theta$ direction comes from the imbalance force due to the eccentricity and hydraulic damping as given below.

$$(m + m_f)(r\ddot{\theta} + 2\dot{r}\dot{\theta}) + c_h|v|r\dot{\theta} = (m + m_f)e_0[\dot{\phi}^2 \sin(\phi - \theta) - \ddot{\phi}\cos(\phi - \theta)] + F_\theta$$

where $F_\theta$ is the tangential force coming from the wellbore when there is a contact. Similarly, torsional acceleration in $\phi$ direction comes from the imbalance torque due to the eccentricity, restoring torque (due to torsional stiffness) and hydraulic and viscous damping as given below.

$$J\ddot{\phi} + k_T(\phi - \phi_{rt}) + c_v\dot{\phi} + c_h|v|\dot{r}e_0 \sin(\phi - \theta) - c_h|v|r\dot{\theta}e_0 \cos(\phi - \theta)$$
$$= -T(x, \phi, \dot{\phi}) + F_\theta[R - e_0 \cos(\phi - \theta)] - F_r e_0 \sin(\phi - \theta)$$

where $T(x, \phi, \dot{\phi})$ is TOB. Equation for torque at the top surface is given by

$$(J_{rt} + n^2 J_m)\ddot{\phi}_{rt} + k_T(\phi_{rt} - \phi) + c_{rt}\dot{\phi}_{rt} - nK_m I = 0$$

where $n$ is the gear ratio. The change in the current in the DC Motor is given by
$$L\dot{I} + R_m I + K_m n\dot{\phi}_{rt} = V_c$$

Finally, axial acceleration in $x$ direction comes from WOB, damping and restoring force (due to axial stiffness) as given below.

$$m_a\ddot{x} + c_a\dot{x} + k_a x = -F(x, \phi) + \bar{F}$$

where $\bar{F}$ is WOB give as
$$\bar{F} = k_a x(0) + F_0$$

where, $x(0)$ is axial displacement at the bit and $F_0$ is applied WOB given as

$$WOB = \begin{cases} k_c(x-s) & if \quad x \geq s, \\ 0 & if \quad x < s, \end{cases}$$

where $s$ is the formation surface elevation given as

$$s = s_0 \sin(n_b\phi)$$

Weight on bit and torque on bit are related non-linearly as given by

$$T(x, \phi, \dot{\phi}) = F(x, \phi)[\mu f(\dot{\phi}) + \varsigma\sqrt{r_h\delta_c}],$$

where $\delta_c$ is the depth of cut per revolution given as

$$\delta_c = \frac{2\pi ROP}{\omega_d}$$

where $ROP$ is the rate of penetration given as

$$ROP = c_1 F_0\sqrt{\omega_d} + c_2$$

where $c_1$ and $c_2$ are constants. The continuous function $f(\dot{\phi})$ used to represent TOB is given as

$$f(\dot{\phi}) = tanh\dot{\phi} + \frac{\alpha_1\dot{\phi}}{1 + \alpha_2\dot{\phi}^2}$$

where $\alpha_1$ and $\alpha_2$ are constants.

## 5.2 Horizontal Drilling System

Horizontal drilling system used in the current study as shown in Figure 19 and Figure 20. The equations for force and torque transmission in horizontal drilling are used from Mohammad [15]. For vertical sections, force balance yields

$$F_2 = F_1 + Static\ Weight \pm \mu F_N$$

where, "1" and "2" represent bottom and top of the drill string element where tension force is applied. For a curved section, force balance as given by [55]

$$F_N = \left[ \left( F_1(\varphi_2 - \varphi_1)\sin\left(\frac{\alpha_2 + \alpha_1}{2}\right) \right)^2 + \left( F_1(\alpha_2 - \alpha_1) + w\sin\left(\frac{\alpha_2 + \alpha_1}{2}\right) \right)^2 \right]^{\frac{1}{2}}$$

The above equation can be used to derive increments in tension and torque as

$$\Delta F = w\cos\left(\frac{\alpha_2 + \alpha_1}{2}\right) \pm \mu F_N$$

$$\Delta T = \mu F_N r$$

The above equations don't take buoyancy into consideration. Hence, we use the following equations instead.
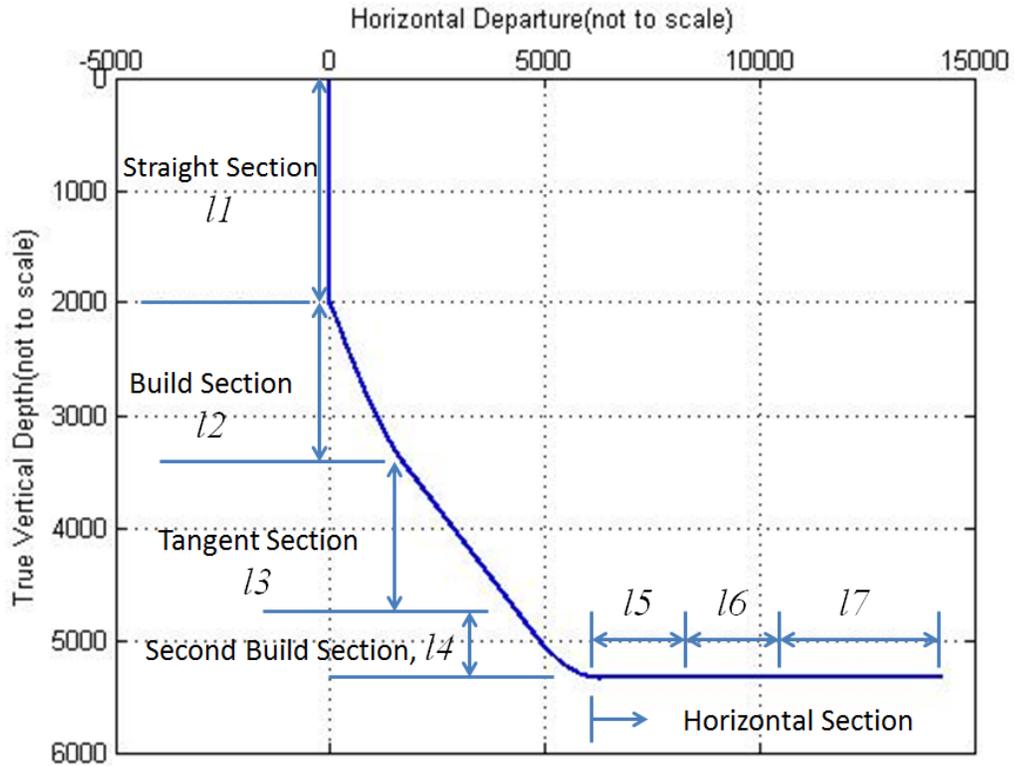
**Figure 19: Horizontal Drilling System Layout**

We define buoyancy factor in order to consider net weight of drill string in a fluid filled well. It is defined as

$$\beta = 1 - \frac{\rho_o A_o - \rho_i A_i}{\rho_{pipe}(A_o - A_i)}$$

Subscripts "o" and "i" refer to outside and inside of drill string.

For straight well bores with inclination $\alpha$,

$$F_2 = F_1 + \beta w \Delta L \{cos\alpha \pm \mu sin\alpha\}$$

"+" is when pipe is pulled upward and "-" when pipe is lowered downward.

If drill string is divided into $n - 1$ elements, then force and torque at the end of the drill string are given by

$$F_n = \sum_{i=2}^{n} \{\beta w \Delta L (cos\alpha \pm \mu sin\alpha)\}_i$$

$$T_n = \sum_{i=2}^{n} \{\beta w \Delta L r sin\alpha\}_i$$

For curved borehole sections,

$$F_2 = F_1 e^{\pm\mu|\theta|}$$

$$T = \mu r N = \mu r F_1 |\theta|$$

For build-up, drop-off, side bends or combination of these,

$$F_2 = F_1 e^{\pm\mu|\theta|} + \beta w \Delta L \left\{ \frac{sin\alpha_2 - sin\alpha_1}{\alpha_2 - \alpha_1} \right\}$$

$$T = \mu r N = \mu r F_1 |\theta|$$

For the entire curved section,

$$F_n = \sum_{i=2}^{n} \left\{ F_{i-1} e^{\pm\mu_i|\theta_i|} + \beta_i w_i \Delta L_i \left( \frac{sin\alpha_i - sin\alpha_{i-1}}{\alpha_i - \alpha_{i-1}} \right) \right\}$$

$$T_n = \sum_{i=2}^{n} \mu_i r_i F_{i-1} |\theta_i|$$

29

BHA modeling in horizontal section is modeled in the same way as that of vertical drilling with an additional gravitational term. The equations are given below.

$$(m + m_f)(\ddot{r} - r\dot{\theta}^2) + k(x, \phi, \dot{\phi})r + c_h|v|\dot{r}$$
$$= (m + m_f)e_0[\dot{\phi}^2 \cos(\phi - \theta) + \ddot{\phi} \sin(\phi - \theta) - g\sin\theta] - F_r$$

$$(m + m_f)(r\ddot{\theta} + 2\dot{r}\dot{\theta}) + c_h|v|r\dot{\theta}$$
$$= (m + m_f)e_0[\dot{\phi}^2 \sin(\phi - \theta) - \ddot{\phi} \cos(\phi - \theta) - g\cos\theta] + F_\theta$$

$$J\ddot{\phi} + k_T(\phi - \phi_{rt}) + c_v\dot{\phi} + c_h|v|\dot{r}e_0 \sin(\phi - \theta) - c_h|v|r\dot{\theta}e_0 \cos(\phi - \theta)$$
$$= -T(x, \phi, \dot{\phi}) + F_\theta[R - e_0 \cos(\phi - \theta)] - F_re_0 \sin(\phi - \theta)$$



Figure 20: Wellbore profile

## 5.3 Rock cutting mechanism

PDC bit has a radius $a$ and gauge $2b$ as shown in Figure 7. Bit/rock interactions are governed by the interface laws from the cutting mechanism (similar to metal cutting process in manufacturing). These interface laws relate the torque-on-bit (TOB) and penetration rate ("the response") to the weight-on-bit (WOB) and the angular velocity ("the input") [44]. There are two types of failure modes- ductile and brittle, in rock cutting. When the depth of cut is shallow, rock fails in ductile mode with continuous diffuse fragmentation of the rock [57]. When the depth of cut is deep, the rock fails in brittle mode through fracture [51]. When the cutting takes place in ductile mode, observations suggest that there exists a bilinear relationship (two regimes) between the forces and cross-sectional area of cut [57]. For larger depths of cut, the cutting process enters in a brittle mode called chipping. Cutting in oil and gas drilling is assumed to be in ductile mode and typically falls into two regimes- regime I and regime II [45].

At the cutter level, two forces- cutting and frictional forces, act on cutting and flank surfaces respectively for a blunt cutter [44] as shown in Figure 21. In case of a sharp cutter, only cutting force acts on the rock as there is no wear flat which causes friction. These forces are given as
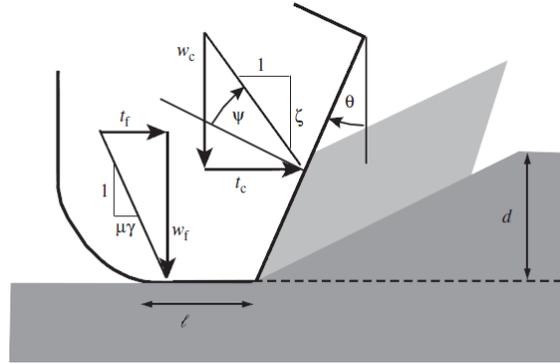


Figure 21: Cutting and frictional components at blunt cutter/rock interface [58]

$$F_s^c = \varepsilon A$$

$$F_n^c = \zeta \varepsilon A$$

$$F_s^f = \mu F_n^f$$

$$F_s = \varepsilon A + \mu F_n^f$$

$$F_s = (1 - \mu\zeta)\varepsilon A + \mu F_n$$

where, $\varepsilon$ is defined as intrinsic specific energy, A is cross-sectional area of the cut, $\zeta$ is the ratio of the vertical to horizontal force acting on the cutting face (ideally, $\zeta = \tan(\theta + \psi)$), $\theta$ back rake angle of PDC cutter, $\psi$ is friction angle at the cutter/rock interface and $\mu$ is coefficient of friction at the wearflat/rock contact.

By integrating individual cutter forces over the bit, torque-on-bit and weight-on-bit for vertical drilling can be expressed as below[44].

$$TOB = TOB^c + TOB^f$$

$$WOB = WOB^c + WOB^f$$

$$TOB^c = \frac{1}{2}\varepsilon\delta a^2$$

$$WOB^c = \zeta\varepsilon\delta a$$

$$\delta = \frac{2\pi v}{\omega}$$

$$\gamma = \frac{2T^f}{\mu a W^f}$$

$$T^f = \frac{1}{2}a\mu\gamma W - \frac{1}{2}a^2\mu\gamma\zeta\varepsilon\delta$$

$$\frac{2T^f}{a} = (1 - \mu\gamma\zeta)\varepsilon\delta a + \mu\gamma W$$

where, a is bit radius, δ is depth of cut per revolution, v is rate of penetration, ω is angular rotation speed of the bit and γ is bit constant. For simplicity, the cutting is assumed to be taking place by two equivalent blades; one at the face and the other at the gauge (face and gauge). Observations suggest that a bilinear relationship (two regimes) exists between the forces and cross-sectional area of cut as shown in the Figure 22. In regime I, both the contact (along the wear flat) and cutting (along the cutting face) forces are proportional to depth of cut p. Whereas in regime II, the contact forces saturate and only the cutting forces keep increasing with depth. The forces per width of cutter are given by the following equations.
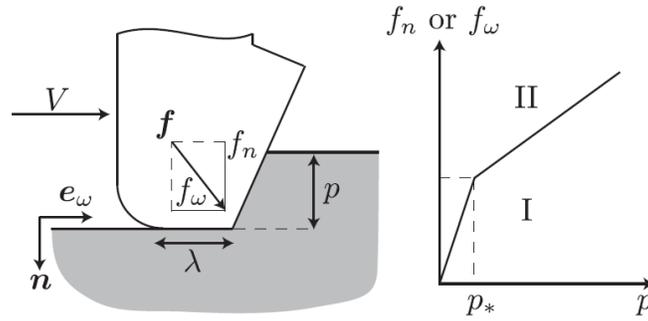


Figure 22: Bilinear laws for a blunt single cutter [45]

$$f_n = \zeta'\varepsilon p, \quad f_w = \zeta''\varepsilon p, \quad p < p_* \quad \text{(Regime I)}$$

$$f_n = \sigma_*\lambda + \zeta\varepsilon p, \quad f_w = \mu\sigma_*\lambda + \varepsilon p, \quad p > p_* \quad \text{(Regime II)}$$

$$\zeta' = \zeta + \frac{\kappa\sigma_*}{\varepsilon}$$

$$\zeta'' = 1 + \frac{\mu\gamma\kappa\sigma_*}{\varepsilon}$$

$$p_* = \frac{\lambda}{\kappa}$$

33

where, $\zeta'$ is a coefficient that defines the normal force in regime I, $\zeta''$ defines the tangent force in regime I, p is the depth of cut, $p_*$ is the critical depth of cut where transition from regime I to regime II happens, $\sigma_*$ is the maximum contact stress at the cutter wearflat, $\lambda$ is the wearflat length, $\kappa$ is the rate of change of contact/wear flat length with depth of cut [58].

Hence, when the axial (face) and lateral (gauge) depths of cut at the bit fall within these two regimes, forces are calculated using the equations above and resultant force vector from all the cutters is calculated.

Drill string is constrained to move in the deviated wellbore structure. The top drill pipe rotates with the speed of the top drive and the bottom part of the collar has the bit angular speed. The stabilizer at the start of the Bottom Hole Assembly (which has drill collars, sensor tools, mud motor, rotor steerable system and bit) maintains contact with the bore wall and helps in Rotary Steerable System(RSS) by acting as fulcrum for push the bit and point the bit mechanisms to maneuver along the desired path. As the stabilizer is in continuous contact with the bore wall, it has only one axial and one torsional motions. Long connection of flexible drill pipes has one axial, one torsional and two lateral degrees of freedom. Drill collar on the other hand acts like an axially moving cantilever beam with the fixed end at stabilizer and bit as the free end.

# 6.   SIMULATION

We consider equal length of horizontal and vertical drill strings for comparison. Simulations for vertical and horizontal drilling systems are performed in MATLAB. Runge-Kutta (RK4) method is used to solve second order differential equations. Hook load of 5150 kN and top rotary speed of 11.5 rad/s were used in the simulations.

## 6.1 Impulse-Momentum Equations

There are six states – $[\theta, \phi, r, \dot{\theta}, \dot{\phi}, \dot{r}]$ as mentioned earlier. Since we have six states, we need three second order differential equations to solve for. These equations (2 Force and 1 Torque balances) of motion of lumped BHA are taken from Christoforou's model [11] given by

$$(m + m_f)(\ddot{r} - r\dot{\theta}^2) + k(x, \phi, \dot{\phi})r + c_h|v|\dot{r}$$
$$= (m + m_f)e_0[\dot{\phi}^2 \cos(\phi - \theta) + \ddot{\phi} \sin(\phi - \theta)] - F_r$$

$$(m + m_f)(r\ddot{\theta} + 2\dot{r}\dot{\theta}) + c_h|v|r\dot{\theta} = (m + m_f)e_0[\dot{\phi}^2 \sin(\phi - \theta) - \ddot{\phi} \cos(\phi - \theta)] + F_\theta$$

$$J\ddot{\phi} + k_T(\phi - \phi_{rt}) + c_v\dot{\phi} + c_h|v|\dot{r}e_0 \sin(\phi - \theta) - c_h|v|r\dot{\theta}e_0 \cos(\phi - \theta)$$
$$= -T(x, \phi, \dot{\phi}) + F_\theta[R - e_0 \cos(\phi - \theta)] - F_r e_0 \sin(\phi - \theta)$$

Three equations are integrated until a contact with the bore wall is detected ($r > \frac{d_h - d_0}{2}$ , where $d_h$ is wellbore diameter and $d_0$ is BHA diameter). When a contact is detected, Impact model algorithm computes the change in state variables and gives new states after the impact. New states are integrated again until the next contact occurs and this process continues. Impact equations are given below.

$$(m + m_f)\Delta\dot{r} = (m + m_f)e_0\Delta\dot{\phi} \sin(\phi - \theta) - P_r$$

$$(m + m_f)r\Delta\dot{\theta} = -(m + m_f)e_0\Delta\dot{\phi} \cos(\phi - \theta) + P_\theta$$

35

$$J\Delta\dot{\phi} = P_\theta[R - e_0\cos(\phi - \theta)] - P_r e_0 \sin(\phi - \theta)$$

where $\Delta\dot{r}$, $\Delta\dot{\theta}$, and $\Delta\dot{\phi}$ are the jump discontinuities in the velocities, and $P_r$ and $P_\theta$ are the impulses of impact forces $F_r$ and $F_\theta$ respectively.

## 6.2 Impact Model

Impact of drill string with the borehole wall is modeled based on Mason and Wang [56]. For an oblique impact, they identified five contact modes: (1) sliding, (2) sticking in compression phase (C-sticking), (3) sticking in restitution phase (R-sticking), (4) reversed sliding in compression phase (C-reversed sliding), and (5) reversed sliding in restitution phase (R-reversed sliding). Impulses are calculated using the following equations.

1.  Sliding: if $P_d > (1+e)P_q$,

$$P_r = -(1+e)\frac{C_0}{B_2 + s\mu B_3}, \qquad P_\theta = -s\mu P_r;$$

2.  C-sticking: if $P_d < P_q$ and $\mu > |\mu_s|$,

$$P_r = -(1+e)\frac{B_1 C_0 + B_3 S_0}{B_1 B_2 - B_3^2}, \qquad P_\theta = \frac{B_3 P_r - S_0}{B_1};$$

3.  R-sticking: if $P_d < P_q < (1+e)P_q$ and $\mu > |\mu_s|$,

$$P_r = -(1+e)\frac{C_0}{B_2 + s\mu B_3}, \qquad P_\theta = \frac{B_3 P_r - S_0}{B_1};$$

4.  C-reversed sliding: if $P_d < P_q$ and $\mu < |\mu_s|$,

$$P_r = -\frac{(1+e)}{B_2 - s\mu B_3}\left[C_0 + \frac{2s\mu B_3 S_0}{B_3 + s\mu B_1}\right], \quad P_\theta = s\mu\left[P_r - \frac{2S_0}{B_3 + s\mu B_1}\right];$$

5. R-reversed sliding: if $P_d < P_q < (1+e)P_q$ and $\mu < |\mu_s|$,

$$P_r = -(1+e)\frac{C_0}{B_2 + s\mu B_3}, \quad P_\theta = s\mu\left[P_r - \frac{2S_0}{B_3 + s\mu B_1}\right];$$

where

$$s = \begin{cases} \dfrac{S_0}{|S_0|} \; if \; S_0 \neq 0 \\ 1 \; if \; S_0 = 0 \end{cases}$$

Here $S_0$ and $C_0$ are the initial values of sliding and compression velocities calculated as

$$S_0 = r\dot\theta + R\dot\phi, C_0 = -\dot r,$$

$B_1$, $B_2$ and $B_3$ are constants which depend on the geometry and mass properties as

$$B_1 = \frac{1}{(m + m_f)} + \frac{[R - e_0\cos(\phi - \theta)]^2}{J}$$

$$B_2 = \frac{1}{(m + m_f)} + \frac{[e_0\sin(\phi - \theta)]^2}{J}$$

$$B_3 = e_0\sin(\phi - \theta)\frac{[R - e_0\cos(\phi - \theta)]}{J}$$

$$P_d = (B_2 + s\mu B_3)sS_0, \quad P_q = -(\mu B_1 + sB_3)C_0, \quad \mu_s = -\frac{B_3}{B_1}$$

37

Here $\mu$ and $e$ are the friction and restitution coefficients, respectively. The coefficient of restitution is given by

$$e = \begin{cases} 1 & if \ \beta \leq 0.893, \\ 0.972\beta^{-\frac{1}{4}} & if \ \beta > 0.893, \end{cases}$$

where $\beta$ is the normalized impact velocity given as

$$\beta = \left( \frac{15.735(m + m_f)(E^*)^4}{\pi 5 \ d_h^3 S_y^5} \right)^{\frac{1}{2}} \dot{r},$$

where $E^*$ is the effective Young's modulus given by

$$\frac{1}{E^*} = \frac{1 - v_1^2}{E_1} + \frac{1 - v_2^2}{E_2},$$

where $v_i$ and $E_i$ are Poisson's ratio and Young's modulus for the drill collars and the formation, respectively, and $S_y$ is the yield strength of the softer material.

# 7.  RESULTS

## 7.1 Weight on bit and torque on bit in Vertical drilling

Vertical drilling model was implemented in MATLAB. Weight on bit is shown in Figure 23. It oscillates around an average weight on bit of about 100 kN. This oscillation is attributed to axial oscillations. As depth of cut decreases, weight on bit decreases and vice versa. When weight on bit is zero, it represents that the bit is no longer in contact with the rock.
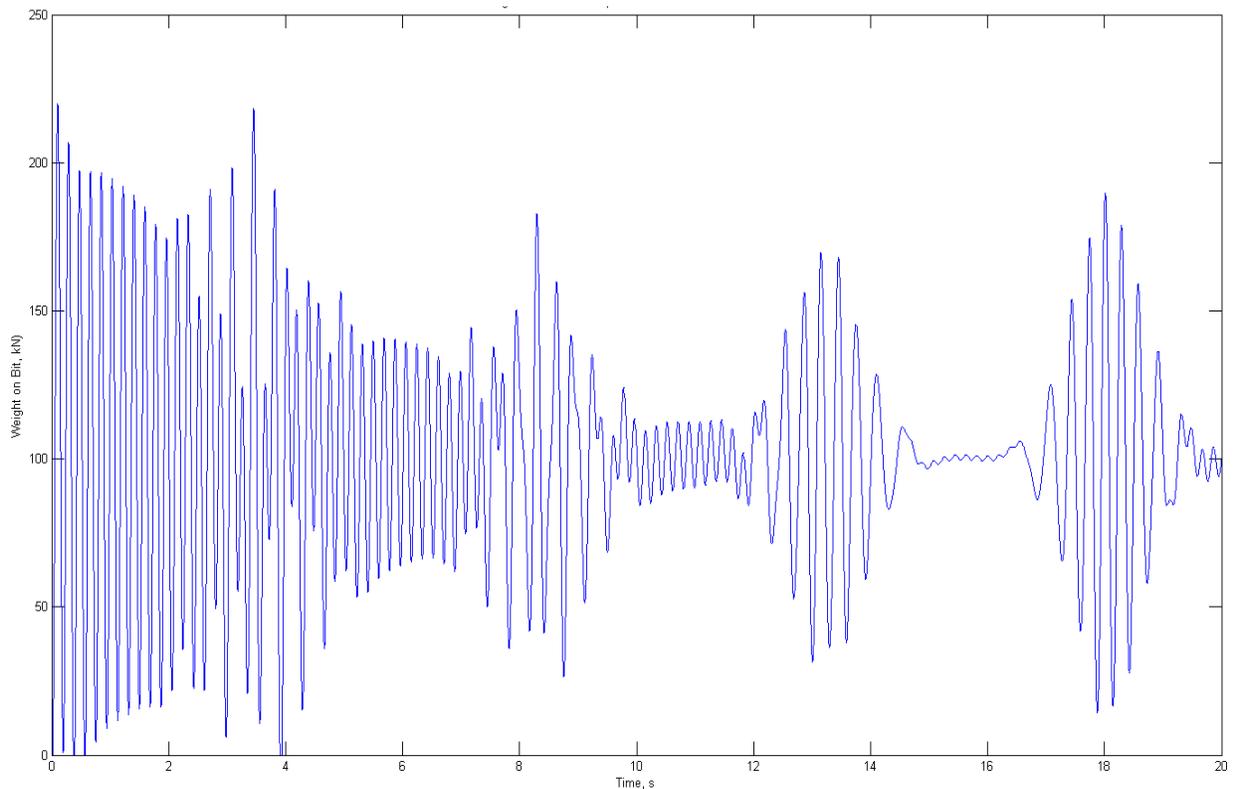


**Figure 23: Weight on bit for vertical drilling**

On the other hand, torque on bit also oscillates in similar patterns to weight on bit as they both are related by equations shown earlier. Torque on bit, as shown in Figure 24, follows top torque but with higher frequency oscillations. Torque on bit oscillates at an average value of 4 kNm.
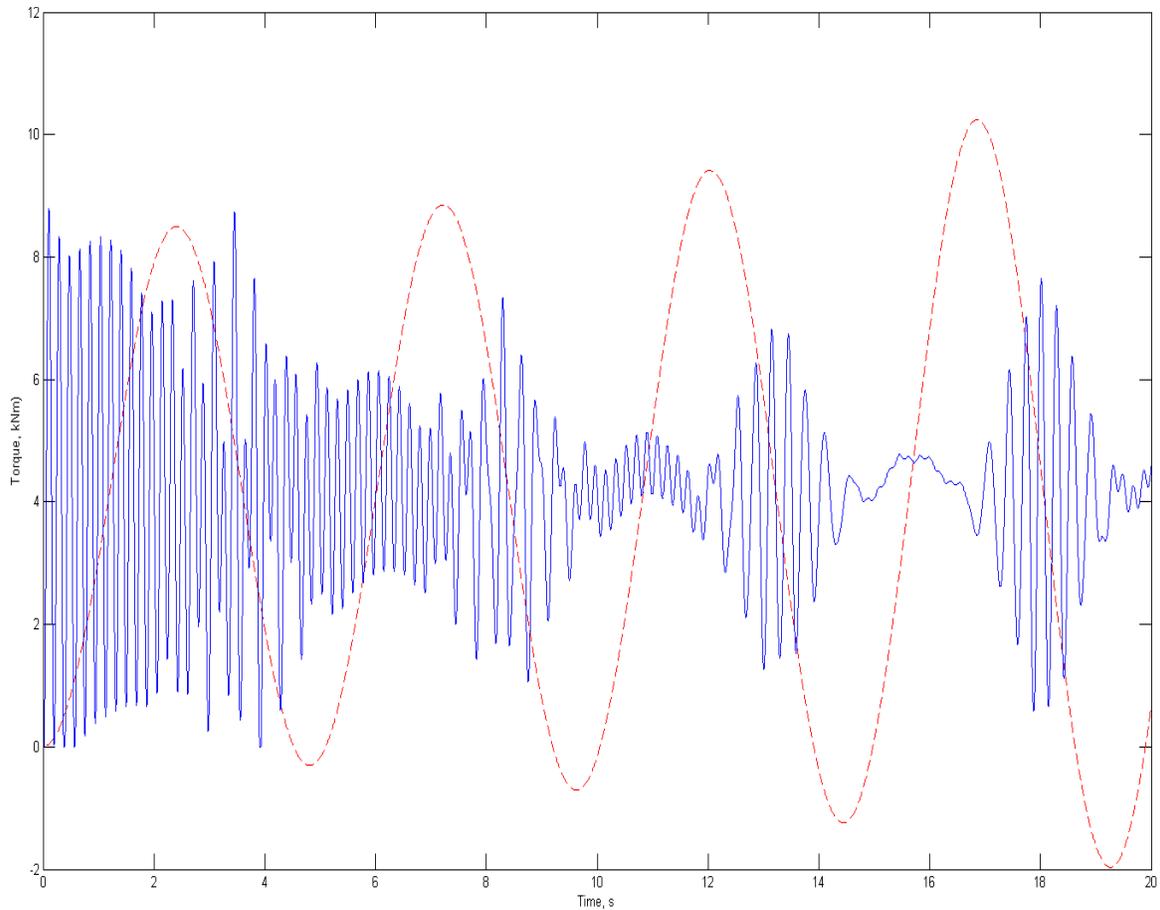
## 7.2 Force and Torque transmission in Horizontal drilling

Based on the formulation as discussed earlier, hook load and top torque are transmitted through the drilling system as weight on bit and torque on bit at the bottom to aid cutting. Hook load at the top is around 7500 kN. From the Figure 25, the lowest force happens at 2000 m where the build-up starts from vertical section. The drill bit experiences weight on bit of about 5150 kN.

40
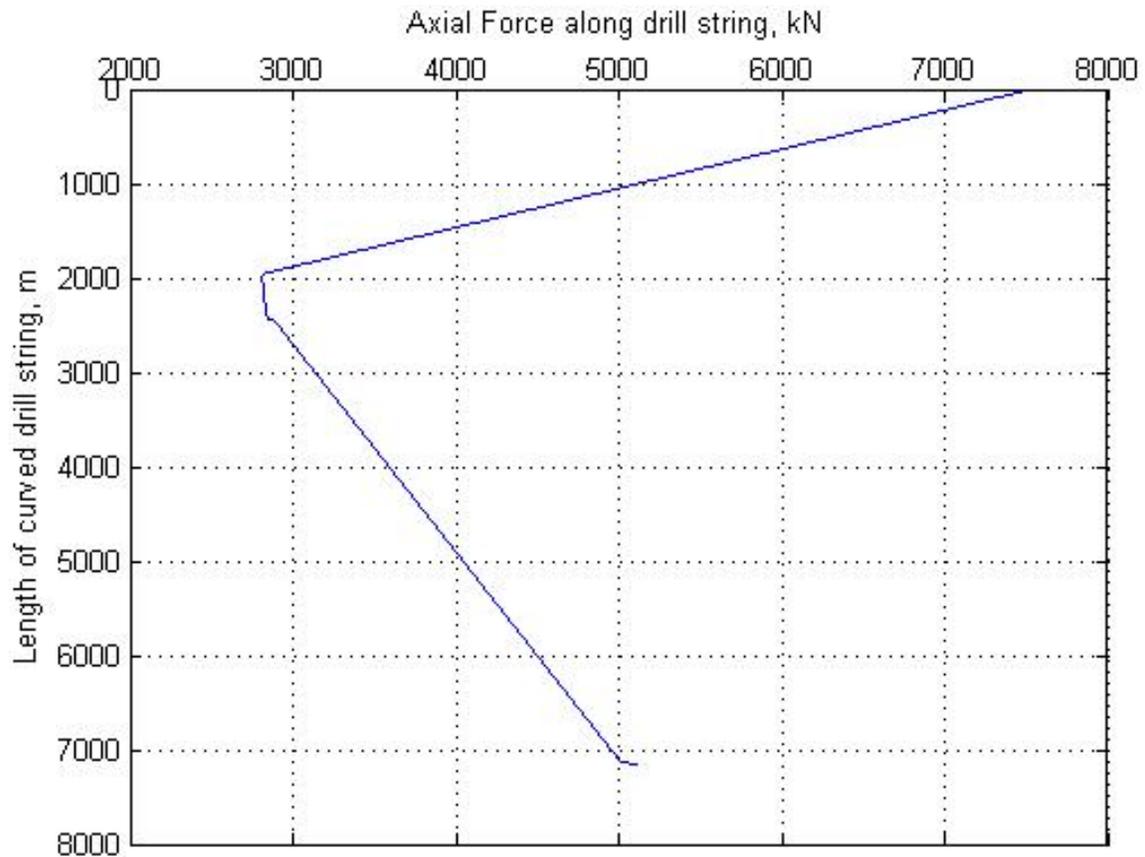
**Figure 25: Force transmission through horizontal drilling system**

Similarly, torque transmission can be seen from the Figure 26. Top torque is around 4 kNm. It remains almost constant in the vertical section and reduces with build-up, hold and horizontal sections. The lowest torque is seen at the bit as torque on bit of about -417 kNm.
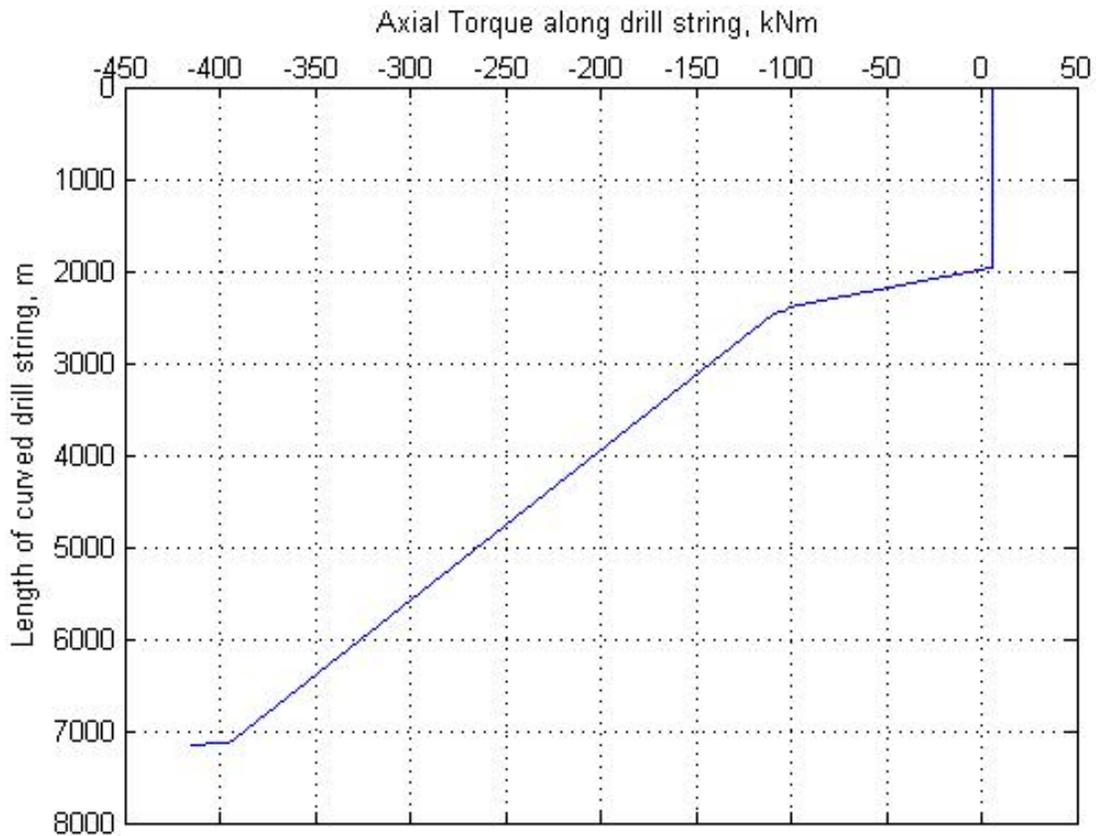
**Figure 26: Torque transmission through horizontal drilling system**

## 7.3 Comparison of vertical and horizontal drilling

Here, the comparison of vertical and horizontal drilling is presented. Top and bit speeds and Top torque and Torque on bit are given for both the cases in Figure 27 and Figure 28.
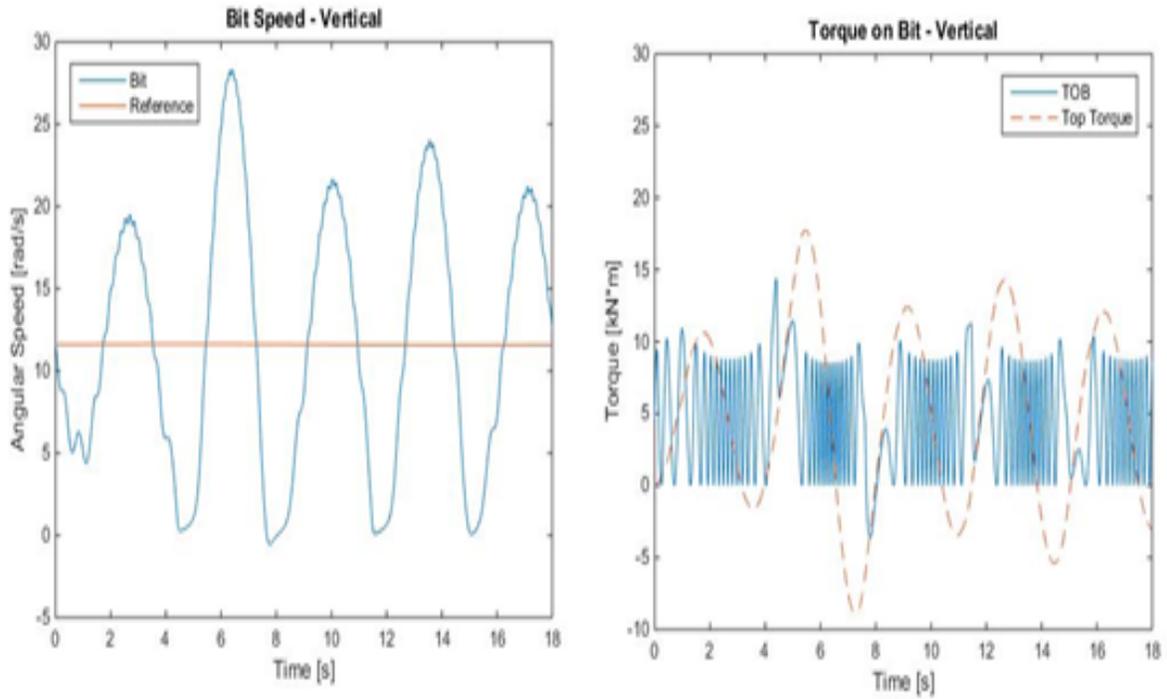
**Figure 27: Bit speed and Torque on bit - Vertical**
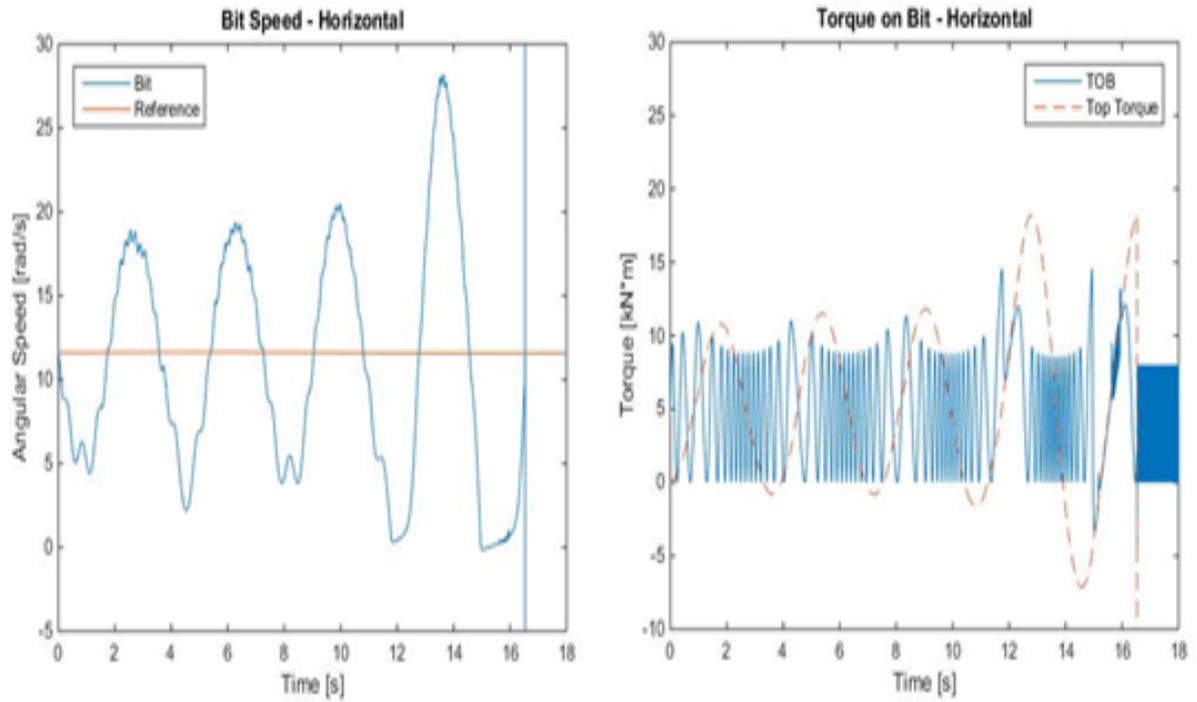


**Figure 28: Bit speed and Torque on bit - Horizontal**

43

# 8.  OBSERVATIONS

The following observations can be made from the results.

1. The constant rotary speed at the top surface doesn't translate into a steady state rotational motion at the bit. There is a stick-slip pattern in the BHA vibrations.
2. Top torque is smooth and has less frequency. Whereas, torque-on-bit fluctuates with a high frequency.
3. We observe pronounced stick slip and torque fluctuations both in horizontal drilling and the vertical drilling case. This is attributed due to the flexibility of drill pipes in torsional direction. We need to look into controlling of stick slip and lateral vibrations as a broad goal. We can reduce torsional and axial vibrations to some extent if we increase the rotational speed at the top surface. Stick-slip occurs at a frequency of 0.25 Hz which is close to field observations.
4. Horizontal drilling becomes unstable after about 16 seconds. Bit speed shoots up really high. Possible causes include the assumptions implemented in the contact model or the integration method. This instability can be attributed to the effect of gravitational force in horizontal drilling which causes high lateral vibrations.

# 9. FUTURE WORK

The following recommendations for future work are suggested.

1. Since horizontal model is not complete, we need to build a comprehensive model which accounts for stabilizers, gyroscopic effects (change in angular momentum), axial stiffening (tension, compression due to gravity), bit/rock interactions, drill string/well bore interactions, fluid damping (both inside and outside of drill pipe), buckling effects: axial, bending and torsional etc. Bit/rock interactions are significant and greatly depend on bit speed and formation stiffness.

2. The model needs to be calibrated by validating with the experimental data. It is also necessary to thoroughly study the magnitudes and frequencies of displacements and forces.

3. We need to perform sensitivity analysis of parameters used in the formulation to build a reduced model for simplicity and low computational time.

4. Validate the assumption of ductile mode of failure mechanism by considering brittle fracture failure. Che's [47] model considers brittle rock and brittle failure mechanism of the rock. Compare both the models (Che [47] and Detournay [44]) to justify the ductile failure assumption.

5. It is also important to know how the borehole is formed (relaxing the bit/borehole tangency constraint). Borehole size is in general larger than the bit size as the bit continuously changes its orientation which results in tilt causing the size of the borehole larger than the bit diameter.

6. Control designs for the proposed model should be studied to steer vibrations away for efficient drilling and prolonged drill string life.

# 10. BIBLIOGRAPHY

[1]. "Key World Energy STATISTICS", International Energy agency, 2015. [Online]. Available: https://www.iea.org/publications/freepublications/publication/KeyWorld_Statistics_2015.pdf

[2]. "Annual Energy Outlook 2015", International Energy agency, 2015. [Online]. Available: http://www.eia.gov/pressroom/presentations/sieminski_04142015.pdf

[3]. "Shale oil and shale gas resources are globally abundant", US Energy Information Administration, January 2, 2014. http://www.eia.gov/todayinenergy/detail.cfm?id=14431

[4]. "Modelling and Analysis of BHA and Drill-String Vibrations", The University of Aberdeen. [Online]. Available: http://www.abdn.ac.uk/engineering/research/projects-138.php

[5]. "EPA says fracking may have polluted groundwater in Wyoming", American City and County, 2011. [Online]. Available: http://americancityandcounty.com/environment/epa-fracking-polluted-groundwater-wyoming

[6]. Alan Petzet, 2009. "BP's Tiber one of industry's deepest wells". Oil and gas Journal Magazine.

[7]. IADC, 2008. "World's longest extended-reach well drilled offshore Qatar". International Association of Drilling Contractors Magazine

[8]. "Horizontal Highlights- Middle East Well Evaluation Review", Schlumberger. Available: https://www.slb.com/~/media/Files/resources/mearr/wer16/rel_pub_mewer16_1.pdf

[9]. E. Detournay, "Center for Engineered Fracturing of Rock," [Online]. Available: http://www.cefor.umn.edu/research/numerical-simulation-tools/directional-drilling/.

[10]. Yigit, A. S., and Christoforou, A. P. 2006. Stick Slip and Bit Bounce Interaction in Oil Well Drillstrings. Journal of Energy Resources Technology 128, 268–274.

[11]. Christoforou, A. P., and Yigit, A. S., 2003. "Fully coupled vibrations of actively controlled drillstrings". Journal of sound and vibration, 267(5), Nov., pp. 1029–1045.

[12]. "Directional terms", Chinook Consulting Services, August 2010. [Online]. Available: http://www.chinookconsulting.ca/News/Directional-drilling-glossary.html

[13]. "Cutting Settling in Deviated Wells Cause Stuck Pipe", Drilling Formulas, 2011. [Online]. http://www.drillingformulas.com/cutting-settling-in-deviated-wells-cause-stuck-pipe/

[14]. Roman J Shor, Mitch Pryor, Eric Van Oort, 2014. "Drillstring Vibration Observation, Modeling and Prevention in the Oil and Gas Industry". DSCC 2014, ASME.

[15]. Mohammad Fazaelizadeh, PhD Dissertation, University of Calgary, 2013. "Real Time Torque and Drag Analysis during Directional Drilling". [Online]. Available: http://theses.ucalgary.ca/jspui/bitstream/11023/564/2/UCalgary_2013_Fazaelizadeh_Mohammad.pdf

[16]. "Drillstring Vibrations and Vibration Modeling," Schlumberger, [Online]. Available: https://www.slb.com/~/media/Files/drilling/brochures/drilling_opt/drillstring_vib_br.pdf.

[17]. "U.S. Rig Count by Type and Target," EnergyEconomist.com, January 1997 - August 21, 2015. http://www.energyeconomist.com/a6257783p/exploration/Detail_Overview.html.

[18]. J. Dunlop, "Increased Rate of Penetration Through Automation," in SPE, Amsterdam, 2011.

[19]. Finne, I., Bailey, J.J., 1960. "An experimental study of drillstring vibration". J. Eng. Ind. - Trans. ASME 82 (2), 129–135.

[20]. Halsey, G.W., Kyllingstad, A., Kylling, A., 1988. "Torque feedback used to cure slip– stick motion". In: SPE 18049, Presented at 63rd Annual Technical Conference and Exhibition in Houston, Texas, Oct. 2–5.

[21]. Apostal, M.C., Haduch, G.A., Williams, J. B., 1990. "A study to determine the effect of damping on finite element based, forced frequency response models for bottomhole assembly vibration analysis". In: SPE-20458, Presented at SPE Annual Technical Conference and Exhibition. New Orleans, LA, USA, pp. 537– 550.

[22]. Spanos, P.D., Payne, M.L., 1992. "Advances in dynamic bottomhole assembly modeling and dynamic response determination". In: SPE 23905, Presented at SPE Drilling conference in New Orleans, Louisiana, Feb. 18–21.

[23]. Brett, J.K., 1992. "The genesis of torsional drillstring vibrations", SPE 21943. J. SPE Drill. Eng., 168–174.

[24]. Dykstra, M.W., Chen, D.C.-K., Warren, T.M., Azar, J.J., 1996. "Drillstring component mass imbalance: a major source of downhole vibrations", SPE 29350. J. SPE Drill. Completion, 234–241.

[25]. Jansen, J.D., van den Steen, L., 1995. Active damping of self excited torsional vibration in oil well drillstring. J. Sound Vib. 179 (4), 647.

[26]. Menand, S., Sellami, H., Tijani, M., Stab, O., Dupuis, D., Simon, C, 2006. Advancements in 3D drillstring mechanics: from bit to the topdrive. In: Proceedings of the SPE-98965, SPE/IADC Drilling Conference. Florida, USA.

[27]. Mihajlovi´c, N., Wouw, N. v. d., Rosielle, P. C. J. N., and Nijmeijer, H., 2007. "Interaction between torsional and lateral vibrations in flexible rotor systems with discontinuous friction". Nonlinear Dynamics, 50(3), Jan., pp. 679–699.

[28]. Navarro-L´opez, E. M., and Cort´es, D., 2007. "Avoiding harmful oscillations in a drillstring through dynamical analysis". Journal of sound and vibration, 307(1-2), Oct., pp. 152–171.

[29]. Navarro-Lopez, E. M., 2009. "An alternative characterization of bit-sticking phenomena in a multi-degree-of-freedom controlled drillstring". Nonlinear Analysis: Real World Applications, 10(5), Oct., pp. 3162–3174.

[30]. Rudat, J., Dmitriy Dashevskiy, J. R. L. P., Dashevskiy, D., and Pohle, L., 2011. "Model-based stability analysis of torsional drillstring oscillations". Control Applications (CCA)

[31]. Liao, C.-M., Vlajic, N., Karki, H., and Balachandran, B., 2012. "International Journal of Mechanical Sciences". International Journal of Mechanical Sciences, 54(1), Jan., pp. 260–268.

[32]. Patil, P. A., and Teodoriu, C., 2013. "A comparative review of modelling and controlling torsional vibrations and experimentation using laboratory setups". Journal of Petroleum Science and Engineering.

[33]. Nandakumar, K., and Wiercigroch, M., 2013. "Journal of Sound and Vibration". Journal of sound and vibration, 332(10), May, pp. 2575–2592.

[34]. A.F.A. Serrarens, M.J.G. van de Molengraft, J.J. Kok and L. van den Steen, H-infinity control for suppressing stick slip in oil-well drillstrings, IEEE Control Systems (1998)

[35]. Yilmaz, M., Mujeeb, S., and Dhansri, N. R., 2013. "A H-infinity Control Approach for Oil Drilling Processes". Procedia - Procedia Computer Science, 20, pp. 134–139.

[36]. Navarro-Lopez, E. M., and Cortes, D., 2007, "Sliding-Mode Control of a MultiDOF Oilwell Drillstring with Stick-Slip Oscillations," Proceedings of the 2007 American Control Conference, New York, IEEE, pp. 3837–3842.

[37]. X. Liu, N. Vlajic, X. Long, G. Meng, B. Balachandran, State-dependent delay influenced drill string dynamics and stability analysis, 9th International Conference on Multibody Systems Nonlinear Dynamics Control, ASME, vol. 7B, 2013, p. V07BT10A065 10.1115/DETC2013-12904

[38]. Fairhurst, "Hard rock drilling techniques," Mine and Quarry Engineering, pp. April 1957, pp 157-161, May 1957, pp 194-197, 1957.

[39]. Zijsling, "Analysis of temperature distribution and performance of polycrystalline diamond compact bits under field drilling conditions," in SPE 59th Annual Conference and Exhibition, Houston, 1984.

[40]. G. D., "Use of single-cutter data in the analysis of PDC bit designs: part I- development of a PDC cutting force model," Journal of Petroleum Technology, pp. 797-849, 1989.

[41]. S. A. Warren T., "Drag bit performance modeling," in SPE Drilling Engineering, 119-L27, June 1989.

[42]. F. R., "Status of polycrystalline-diamond-compact bits: part 1- development," Journal of Petroleum Technology, pp. 675-684, June, 1988.

[43]. F. R., "Status of polycrystalline-diamond-compact bits: part 2- applications," Journal of Petroleum Technology, pp. 817-821, July, 1988.

[44]. E. Detournay, "A phenomenological model for the drilling action of drag bits," International Journal of Rock Mechanics and Mining Sciences & Geomechanics Abstracts, 1992.

[45]. Downton, "Bit rock interface laws in directional drilling," International Journal of Rock Mechanics and Mining Sciences, pp. 81-90, 2012.

[46]. E. D. Julien Marck, "Spiraled boreholes an expression of 3D directional instability of drilling systems," in SPE/IADC, London, UK, 2015.

[47]. K. F. E. Demeng Che, "Polycrystalline Diamond Turning of Rock," in ASME 2013 International Manufacturing Science and Engineering Conference, Madison, 2013.

[48]. Y. Nishimatsu, "The mechanics of rock cutting," International Journal of Rock Mechanics and Mining Sciences, pp. 9(2), pp. 261-270, 1972.

[49]. L. Gerbaud, "PDC Bits: All comes from the cutter rock interaction," in SPE/IADC, Miami, 2006.

[50]. Akbari, "Dynamic Single PDC Cutter Rock Drilling Modeling and Simulations Focusing On Rate of Penetration Using Distinct Element Method," in ARMA, San Francisco, 2011.

[51]. Y. Zhou, "Numerical Modeling of Rock Drilling with Finite Elements," University of Pittsburgh, 2013.

[52]. G. D., "Use of single-cutter data in the analysis of PDC bit designs: part I- development of a PDC cutting force model," Journal of Petroleum Technology, pp. 797-849, 1989.

[53]. D. Che, "Issues in Polycrystalline Diamond Compact Cutter-Rock Interaction from a Metal Machining Point of View-Part I: Temperature, Stresses, and Forces," Journal of Manufacturing Science and Engineering, vol. 134, pp. 064001-1 to 064001-10, 2012.

[54]. Dykstra. J, Zhijie, V. Madhu, X. Yuzhen, "Dynamic Modeling of Bottomhole Assembly". DSCC 2014, ASME.

[55]. Johancsik, C. A., Friesen, D. B. and Dawson, R., "Torque and Drag in Directional Wells Prediction and Measurement", Journal of Petroleum Technology, June 1984.

[56]. Y. Wang and M. T. Mason 1992, American Society of Mechanical Engineers Journal of Applied Mechanics 59, 635–642. "Two-dimensional rigid-body collisions with friction".

[57]. L. Perneder, "A Three-Dimensional Mathematical Model of directional drilling," The University of Minnesota, 2013.

[58]. E. Detournay, "Response of drag bits: Theory and experiment," International Journal of RockMechanics & Mining Sciences, p. 45 (2008) 1347–1360, 2008.